



Astronomical Time Scale for the Mesozoic

Chunju Huang

State Key Laboratory of Biogeology and Environmental Geology, School of Earth Sciences, China University of Geosciences, Wuhan, China

E-mail: huangcj@cug.edu.cn

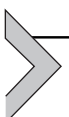
Contents

1. Introduction	82
2. Astronomical Theory and the 405-kyr Astronomical Tuning	83
2.1 Astronomical Theory	83
2.2 The 405-kyr Astronomical Tuning	87
3. The Current Status of the Triassic ATS	90
3.1 The Early Triassic	90
3.2 The Middle Triassic	94
3.3 The Late Triassic	99
4. The Current Status of the Jurassic ATS	104
4.1 The Early Jurassic	104
4.2 The Middle Jurassic	111
4.3 The Late Jurassic	115
5. The Current Status of the Cretaceous ATS	118
5.1 The Early Cretaceous	118
5.2 The Late Cretaceous	126
6. Conclusions	138
Acknowledgments	138
References	138

Abstract

The astronomical theory and its application to sediment cyclostratigraphy have been widely studied over the past thirty years. Especially during the past decade, these have been successfully applied for a continuous high-resolution calibration of portions of the geologic time scale. The method of astronomical tuning enhances the traditional geological dating methods, such as paleontology, paleomagnetism and radioisotope dating. In *The Geologic Time Scale 2012* (GTS2012), most of the Cenozoic Era was directly calibrated to the absolute astronomical time scale

(ATS); however, only a few intervals of the Mesozoic-Paleozoic were scaled by cyclostratigraphy in discontinuous floating segments. Since then, other cyclostratigraphy studies have been published using the most stable 405-kyr long-eccentricity cycle to calibrate portions of the Mesozoic geological time scale. Other than some gaps within the mid-Triassic and Middle Jurassic, it is possible to compile a nearly complete ATS status for the Mesozoic. This chapter compiles and recalibrates an extensive suite of selected paleoclimate proxies series and applies a tuning to the master astronomical scale based on the stable 405-kyr long-eccentricity period. This enables the synthesis of a nearly complete Mesozoic ATS to the base of the Triassic.



1. INTRODUCTION

An accurate geological time scale is the essential key for understanding and deciphering the Earth's evolutionary history and geologic processes. The age model for the geologic time scale with integrated biostratigraphy, chemostratigraphy and magnetostratigraphy that we currently use was constructed largely based on only a few age calibrations from radioisotope dating (Gradstein, 2012). However, a high-resolution age model is not always available or only vaguely defined for many stratigraphic sections (Hinnov and Hilgen, 2012). For example, until recently, due to a lack of precise dating, it was debated whether the major end-Permian mass extinction event was instantaneous in different ecosystems or how it was associated with different stages of the Siberian large igneous province (e.g., Benton and Twitchett, 2003; Shen and Bowring, 2014; Burgess et al., 2014; 2017; Shen et al., 2018). In addition, most of the isotopic dates are not located at the geological stage boundaries. The compilation of *The Geologic Time Scale* (GTS2012) is one of the most important reference books for the geoscience community that provided the current status of an integrated time scale; however, its main framework for the associated age model for the set of geologic stages and primary biozonations of chronostratigraphic units was largely constructed by different interpolation methods of uncertain precision (Gradstein, 2012). Astronomical tuning of the orbital forced stratigraphic records to construct the high-resolution Astronomical Time Scale (ATS) can be developed to solve this problem. In GTS2012, this was applied for a full astronomical calibration of the Quaternary, Neogene and most of Paleogene periods (Hinnov and Hilgen, 2012).

For pre-Cenozoic intervals, the astronomical signals in the cyclic stratigraphic records could not be calibrated directly to an absolute ATS due to

model limitations and uncertainties on the full orbital solution and the lack of a continuous cyclic sediment record connecting to the base of the Cenozoic. Nonetheless, it has been possible in numerous cyclostratigraphic studies to develop “floating” time scales for portions of the Mesozoic and Paleozoic eras based on recognition and tuning of the sediment records to different Milankovitch orbital periods (e.g., short- or long-eccentricity, obliquity and/or precession). Applying shorter orbital periods for tuning has an inherent uncertainty in that minor hiatuses or ambiguities in the sediment record can easily result in omission or non-recognition of one or more cycles. Indeed, any cyclostratigraphy is generally considered to be a minimum estimate of the actual duration.

However, the 405-kyr long-eccentricity period is often present in the deep time sedimentary records and this term is much more stable than the ~100-kyr short-eccentricity or other orbital terms (Laskar et al., 2011), therefore it has been proposed as the primary “metronome” for establishment of geological timescales (Laskar et al., 2004; Hinnov and Hilgen, 2012). In order to construct the high-precision ATS for the Mesozoic Era based on the 405-kyr long-eccentricity tuning, we need apply the uniform standards for the astronomically calibration of continuous cyclostratigraphic records that span major intervals of geologic time and contain records of global biostratigraphic, chemostratigraphic or magnetostratigraphic zones and events. Even though this chapter mainly presents the estimates of ages and durations of international geologic stages, the main goal of cyclostratigraphy and the ATS is determining the actual rates and precise relative and absolute timing of the succession of evolutionary, geomagnetic, geochemical and other events through Earth’s history.



2. ASTRONOMICAL THEORY AND THE 405-KYR ASTRONOMICAL TUNING

2.1 Astronomical Theory

A major paleoclimate factor is the difference between summer warmth and winter cooling at a given latitude, which in turn are largely governed by the difference in the amount of solar radiation (insolation) received through the year at that latitude. For example, a continental ice sheet will grow and advance if the amount of summer heat is inadequate to completely melt the snow that accumulated during the winter. The mean seasonal insolation received at different latitudes on the Earth’s

surface are gradually changing due to slow cyclic variations in the magnitude and in the direction of the Earth's rotational tilt relative to the Sun (obliquity and precession) and in the magnitude of Earth's elliptical orbit around the Sun (eccentricity). Milutin Milanković, a Serbian mathematician and atmospheric scientist, was the first to compute Earth's insolation parameters for a given season and latitude and proposed that long-climate responded to these "Milankovitch" orbital forcings (Milankovitch, 1941). His computation of insolation quantities on Earth has been enhanced by Laskar et al. (1993, 2004, 2011) to provide us an astronomical solution or Astronomical Time Scale (ATS) spanning from 250 million years (Myr) in the past and 250 million years in the future. However, Laskar's current solution is valid for calibrations of paleoclimatic data from all the contributions only for the past/future 50 million years. Beyond this time, the solution's accuracy decreases for some components, especially the precision for the exact ages of maximum precession and obliquity, due to chaotic behavior in the gravitational interaction of the planets and minor planets and tidal-induced exchange of energy between the Earth and Moon (Laskar et al., 2011).

The Earth's main orbital parameters, also known as Milankovitch cycles, are the precession, obliquity and eccentricity cycles and their long-term modulation. The most important for causing seasons on the Earth is its tilt relative to the Sun, because if the Earth was not tilted, then there would not be any significant seasonal change at any latitude. The Earth's orbital obliquity or axial tilt (ϵ) is the angle between the Earth's equatorial plane and its orbital plane, or the angle between an Earth's rotational axis and its orbital axis (Berger and Loutre, 2004). The current obliquity ϵ_0 is 23.44° , and the obliquity oscillates between 22.5° and 24.5° and will be progressively decreasing during the next 10 ka. The principal period of obliquity cycles are 41 kyr, with lesser cycles at 54, 39.5 and 29 kyr for the time interval 0–5 Ma. Due to the tidal dissipation interactions of the Earth and Moon, the periods for obliquity oscillation were more rapid in the past. During the early Triassic (244–249 Ma), the principal period was 34.5 kyr, and less ones were 33.6, 43 and 26 kyr (Fig. 1B).

Precession of the axial tilt relative the Earth's elliptical orbit around the Sun magnifies the seasonal contrast for a hemisphere. Today, the northern hemisphere is closer to the Sun during its winter season than during its summer season. The definition of the Earth's orbital precession parameter is $e \cdot \sin(\varpi)$, where ϖ is the Earth's spin rate and e is the eccentricity. Due to the dissipative effects of the Earth-Moon system, the Earth rotation

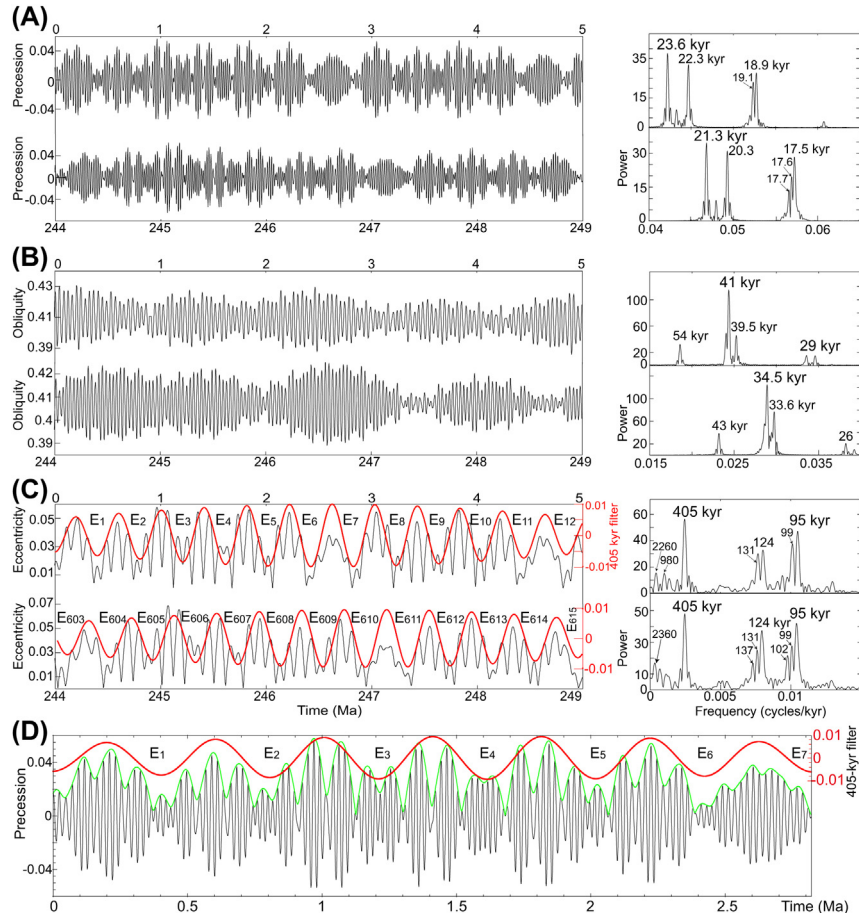


Figure 1 The La2010d nominal solution of Earth's orbital parameters for the past 0–5 Ma and for the Early Triassic (244–249 Ma) (Laskar et al., 2011). (A) Precession index time series for 0–5 and 244–249 Ma with its power spectrum on the right. (B) Obliquity time series for 0–5 and 244–249 Ma with its power spectrum on the right. (C) Eccentricity time series with 405 kyr filter output for 0–5 and 244–249 Ma with its power spectrum on the right. (D) precession index (black curve) for 0–2.82 Ma modulated by eccentricity time series (green curve (gray in print version)) with 405 kyr filtered output. Labels on spectral peaks indicate periodicity in kyr. The 405 kyr filtered curve used a Gaussian filter centered at 0.002469 with passband ± 0.0003 in the AnalySeries 2.0.8 software package (Paillard et al., 1996).

rate is slowing down and the Earth-Moon distance is increasing. This causes both a significant change in the length of day (e.g., it was only 22 h during the early Triassic, 250 Ma) and a slowing of the precession cycle. At present, the main periods of precession cycles are 23.6, 22.3, 19.1 and 18.9 kyr,

however, during the early Triassic the main periods were 21.3, 20.3, 17.7, 17.6 and 17.5 kyr (Fig. 1A).

The amplitude of precession signal on climate is strongly modulated by the magnitude of eccentricity of Earth's elliptical orbit; if the Earth's orbit was circular around the Sun, then its precession cycle would not change the seasonal contrasts through that cycle. The Earth's orbital eccentricity e (a measure of the degree of ellipticity of the Earth's orbit around the Sun, in which a value of "0.0" is circular) is currently 0.016 (Laskar et al., 2004). The interaction of the Earth with the gravitational pull of the other planets causes the eccentricity to vary between 0.00021318 and 0.066957 with the main periods being 95, 99, 124, 131, 405, ~ 1 and ~ 2.3 Myr (Fig. 1C). The amplitude variations of the precession cycles are modulated by the ~ 100 -kyr short-eccentricity cycles, and the amplitude of ~ 100 kyr cycles are modulated by the 405-kyr long-eccentricity cycles (Fig. 1D). The ~ 100 and 405 kyr periods remain quite stable through geologic time, especially 405-kyr long-eccentricity cycle. Indeed, due to the huge mass of Jupiter and the gravitational interactions between the orbital perihelia of Venus and Jupiter, the 405-kyr long-eccentricity cycle has remained stable in the past 250 Myr and is less influenced by the Solar system's chaotic diffusion than the frequency for the ~ 100 -kyr short-eccentricity cycle (Laskar et al., 2004; 2011).

These cyclic variations of the Earth's orbit around the Sun govern the seasonal insolation received at a latitude on the Earth's surface, thereby driving cyclical fluctuations of the climate system. The record of these periodic fluctuations of climate can be preserved by proxies of temperature, runoff, productivity, current intensity or other climatic-sensitive features within the sedimentary deposits to produce rhythmic cycles superimposed on longer-term sediment trends. Extracting these cyclic variations in preserved climatic proxies and determining if they were induced by a suite of Milankovitch orbital cycles is the goal of cyclostratigraphy. Once the main climatic cycle signals are extracted and proven to be associated with certain Milankovitch cycles, then the period of those cycles can be applied to the sediment record to convert the meter-record into a time-record. This astronomical tuning from the depth domain into a time domain often enables the resolution of additional climatic cycles that correspond to additional major Milankovitch cycles.

2.2 The 405-kyr Astronomical Tuning

The astronomical tuning method to assign a certain time scale for the recognized astronomical cycles recorded in a sedimentary succession leads to the construction of a tentative Astronomical Time Scale (ATS) for that sedimentary succession (Hilgen, 2010; Hinnov and Hilgen, 2012), which under ideal conditions can be directly matched to the astronomical solution for absolute age assignments. This process of progressive tuning, development of ATS segments and calibration to the full orbital solution has enabled the construction of a precise Neogene through Quaternary time scale. Calibration to the eccentricity components of the orbital solution underpins the majority of the current Paleogene time scale.

This discipline of cyclostratigraphy to study the cyclic stratigraphic records to search for Milankovitch cycles uses climate proxies such as carbon and oxygen isotopes, depositional facies, magnetic susceptibility, carbonate content, total organic carbon (TOC), grayscale, well logs, etc. The most stable cycles are those of eccentricity, especially 405-kyr long-eccentricity cycle, which are commonly signals superimposed on the geological sedimentary succession. Examples of different proxies and different Mesozoic sedimentary successions include a grayscale series from Cretaceous pelagic sediments in the Piobbico core of central Italy (Fig. 2A), a TOC content series from the Jurassic hemipelagic sediment in a borehole from Dorset, England (Fig. 2C), and relative-depth rank series from Triassic lacustrine deposits cored in the Newark Basin (USA) (Fig. 2E). In each of these depositional settings, the 405-kyr long-eccentricity cycles are well preserved even they have different thickness and facies characteristics (Fig. 2BDF).

The 405-kyr long-eccentricity cycle is the most stable period among the Earth's orbital parameters and has been called the 405-kyr metronome for geologic time. Therefore, we chose this 405 kyr term as a chrono-cycle for calibrating the Mesozoic geologic time scale and designated the chrono-cycle scale from E163 at the Cretaceous/Paleogene boundary (66 Ma) to E622 at the Permian/Triassic boundary (251.9 Ma) (Fig. 1). The goal of the Cyclostratigraphy Research Working Group of International Stratigraphic Commission is trying to identify each of these 405-kyr long-eccentricity cycles in the sedimentary geologic records throughout Phanerozoic. The long-term goal is to assign the appropriate 405-kyr chrono-cycles to biozones, magnetic chronos and other stratigraphic intervals (Hinnov and Hilgen, 2012).

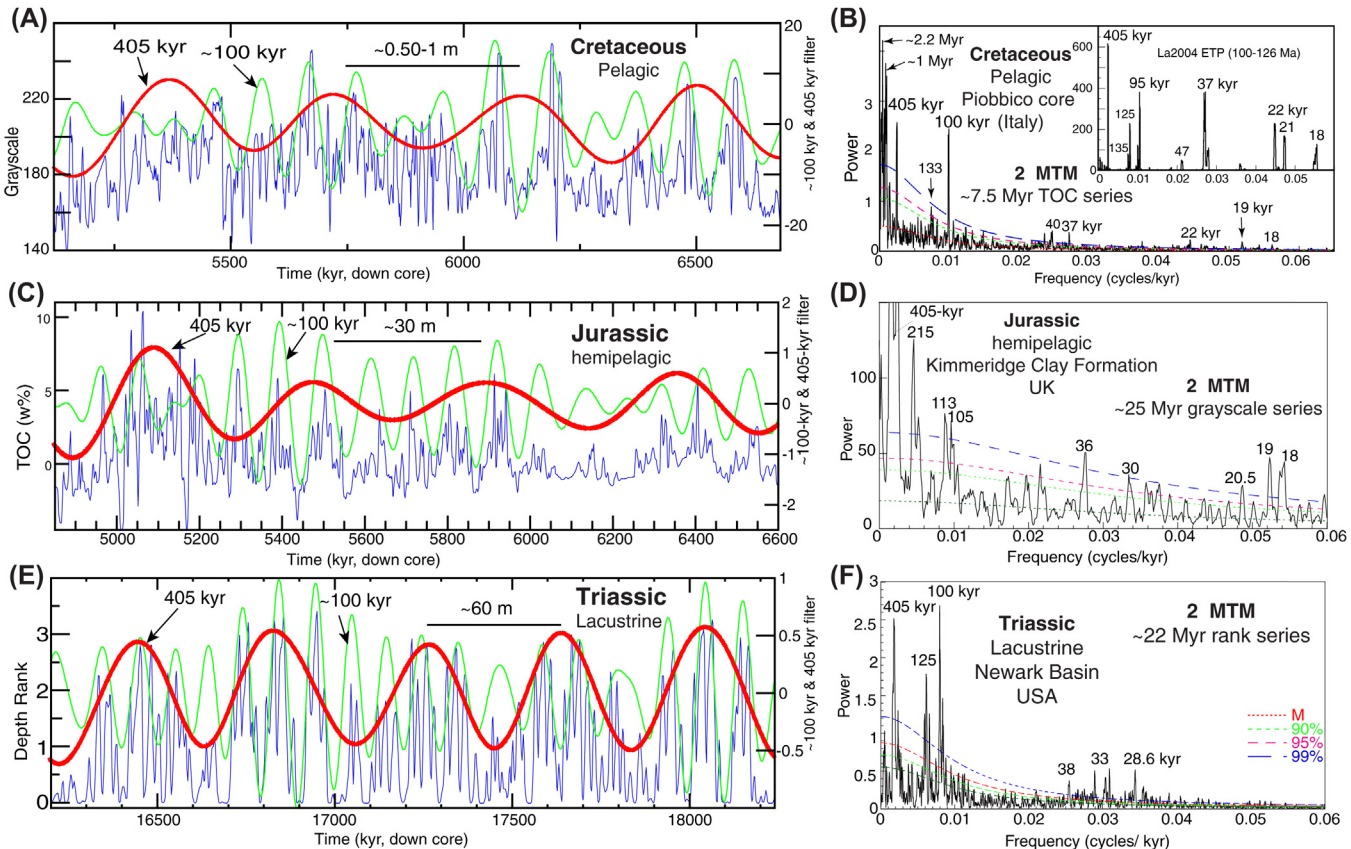
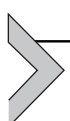


Figure 2 The dominant 405-kyr long-eccentricity cycles recorded in different facies and different paleoclimate proxies in the Mesozoic. (A) An example interval of the grayscale series of the pelagic facies in the Piobbico core (central Italy) of the Aptian Stage of Early Cretaceous with ~ 100 kyr and 405-kyr short and long-eccentricity filter output. (B) 2π multitaper (MTM) power spectrum of the 405 kyr tuned grayscale 25.85 Myr-long ATS for the Piobbico core. (C) An example interval from the TOC content series from the hemipelagic Kimmeridge Clay Formation of Dorset (England) of Late Jurassic. (D) 2π multitaper (MTM) power spectrum of the 405 kyr tuned 7.5 Myr-long TOC ATS for the Kimmeridge Clay Formation. (E) An example interval for the lacustrine depth rank series of Newark Basin (USA) of Late Triassic. (F) 2π multitaper (MTM) power spectrum of the 405 kyr tuned ~ 22 Myr-long depth rank ATS for the Newark composite cores. ~ 100 and 405 kyr filter output using the Gaussian filter, passband at 0.01 ± 0.003 and 0.002469 ± 0.00006 cycles/kyr, respectively.

These 405-kyr long-eccentricity chrono-cycles have an estimated cumulative uncertainty of ~ 500 kyr at 250 Ma for calibrating the geologic time scale (Hinnov and Hilgen, 2012). As noted above, the 405-kyr long-eccentricity cycles are very often present in many Mesozoic stratigraphic records, even where the short periods signals, such as obliquity or precession cycles and even ~ 100 -kyr short-eccentricity cycle, may not be clearly visible or resolved in the ancient stratigraphic sequences. Therefore, the stable 405-kyr long-eccentricity cycle should be used to calibrate the Mesozoic and Paleozoic time scale (Laskar et al., 2004; Hinnov and Hilgen, 2012). Several intervals with astronomically calibrated “floating time scales” have been used for partial calibration of events and zone durations within intervals in the GTS2012 (Gradstein, 2012). In this chapter, we assemble and standardize the analysis of large portions of the available data from those and later cyclostratigraphy studies in order to apply 405-kyr long-eccentricity tuning. These 405-kyr-tuned intervals are assigned to potential 405-kyr chrono-cycles in Mesozoic Era.



3. THE CURRENT STATUS OF THE TRIASSIC ATS

The Triassic period is bounded by end-Permian and end-Triassic mass extinctions. There are U-Pb dates of 251.902 ± 0.024 Ma at the Permian/Triassic boundary (PTB) (Burgess et al., 2014) of 201.36 ± 0.17 Ma at the Triassic/Jurassic boundary (revised by Wotzlaw et al., 2014 from 201.31 ± 0.18 Ma in Schoene et al., 2010); therefore, the Triassic spans a total duration of about 50.5 Myr. The bases of the 7 international Triassic stages as assigned at GSSPs or at candidate definitions are at levels corresponding to the lowest occurrences of ammonoid or conodont taxa within exposures in Alpine, Mediterranean or Himalayan exposures (e.g., reviews in GTS2012 and in Ogg et al., 2016). Over 30 cyclostratigraphic studies have been published for the Triassic in the past three decades (Fig. 3).

3.1 The Early Triassic

The Early Triassic includes **Induan** and **Olenekian stages** and spans about 5 Myr from ~ 252 Ma at Permian/Triassic boundary (PTB) to ~ 247 Ma at Early/Middle Triassic boundary.

Astronomically-forced stratigraphic records through the PTB interval have been proposed by several researchers with differing conclusions

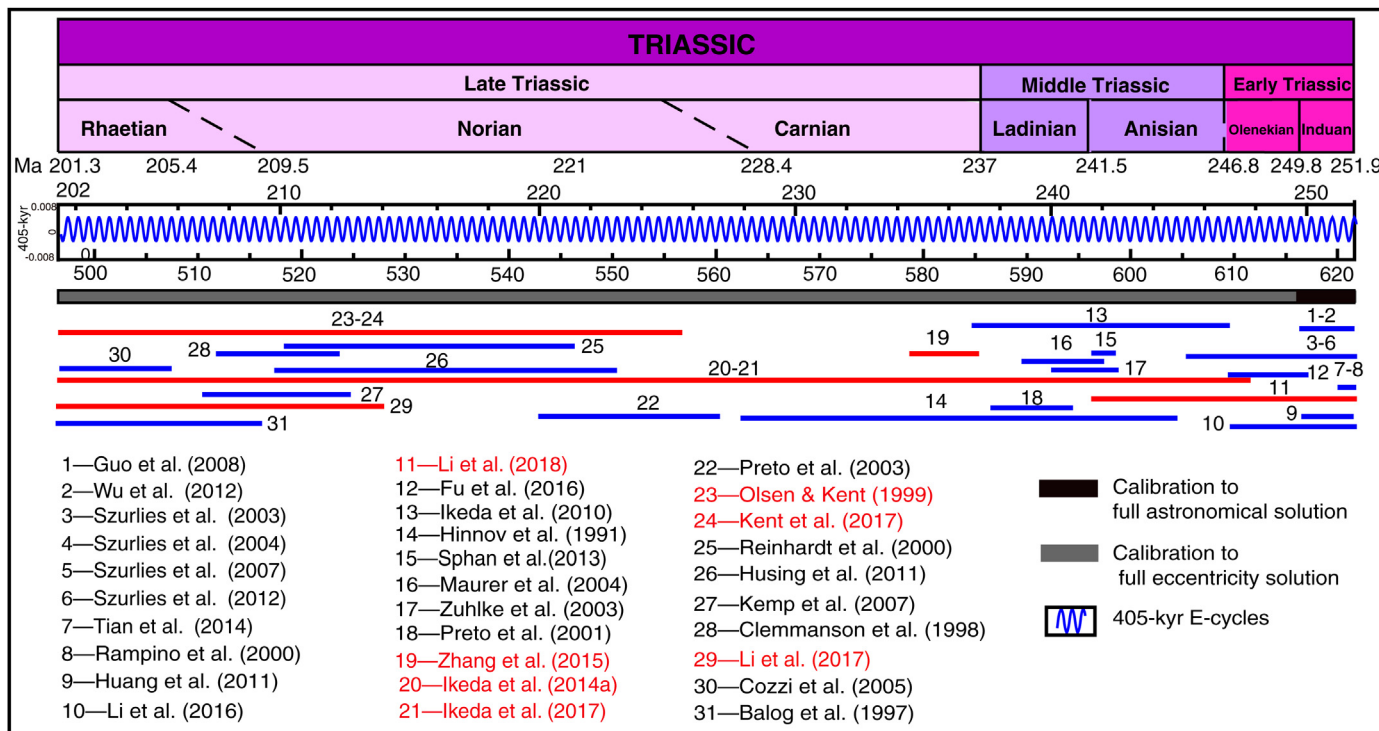


Figure 3 Stratigraphic coverage of the Triassic ATS and 405-kyr metronome. Intervals with *red lines* (gray in print version) indicate the collected data coverage subjected to a 405 kyr tuning to compile the ATS in this study, and those with *blue lines* (dark gray in print version) indicate additional supporting cyclostratigraphy studies.

(Algeo et al., 2010; Hansen et al., 2000; Huang et al., 2011; Rampino et al., 2000; Tian et al., 2014; Yin et al., 2001).

The Induan Stage has been studied in Europe and in South China. In the Carnic Alps in Austria, Rampino et al. (2000) interpreted Milankovitch cycles for the PTB and the basal Griesbachian substage of the Induan from the 331 m Gartnerkofel-1 core that mainly consisted of cyclic dolomitized limestones and interbedded thin marls/shales of shallow-marine facies. Power spectrum of the stacked normalized gamma-ray and density logging data shows ~ 36 , ~ 11 , ~ 4.7 and ~ 2.2 m cycles with a ratio of $\sim 40:10:4.7:2.2$ that is approximately correlative to the ratio $\sim 400:100:37:19$ for the Late Permian astronomical parameters (Berger., 1988). Using a count of the dominant ~ 100 -kyr short-eccentricity cycles, the estimated total duration for the Griesbachian substage was about ~ 1.6 Myr (Rampino et al., 2000). In contrast, a much shorter duration was interpreted at the West Pingdingshan section of Chaohu, Anhui province of South China by Guo et al. (2008), who collected 2184 samples for the magnetic susceptibility (MS) data measurement from the 44 m succession of limestone cyclicly interbedded with mudstone. His interpretation of 56 precession and 12 short-eccentricity cycles implied that the entire Induan Stage spanned only 1.1 Myr. From the Daxiakou section of Hubei province in South China, Wu et al. (2012) interpreted a similar Induan duration of 1.16 Myr based on tuning the 55 m MS and anhysteretic remanent magnetization (ARM) series (2440 samples) to 405, 100 and 20 kyr cycles.

For the Olenekian Stage, Fu et al. (2016) collected high-resolution carbonate carbon-isotope $\delta^{13}\text{C}_{\text{carb}}$ data from the slope-facies succession in the 200 m Majiashan section at Chaohu in South China. They interpreted a 3.2 Myr-long ATS for the late Smithian through Spathian of Olenekian stage, of which the Spathian substage spanned an estimated 2.89 Myr duration based on assigning a 115.3-kyr short-eccentricity tuning to the observed main cycles. Their age model assumed that $\delta^{13}\text{C}_{\text{carb}}$ minima correspond to long-eccentricity maxima and an anchor at a horizon of 162.62 m to the eccentricity curve of La2010d at 247.95 Ma. Their interpretation was partly influenced by the estimated duration of 3.2 ± 0.6 Myr from a pair of earlier U-Pb radioisotopic dates of 250.55 ± 0.51 Ma for the earliest Spathian (Ovtcharova et al., 2006) and 247.32 ± 0.08 Ma for the end-Spathian (Lehrmann et al., 2006). The end-Spathian U-Pb date has been partly independently verified in another

section (Ovtcharova et al., 2015), but the interpreted U-Pb date for earliest Spathian has yet to be verified.

Those estimates of a short-duration Induan Stage and a long-duration Olenekian Stage (especially for the Spathian substages) are very different than those derived from extensive cycle–magnetostratigraphy correlation in Europe and to South China. Szurlies et al. (2003, 2012) and Szurlies (2004) interpreted ~ 100 -kyr short-eccentricity cycles from outcrops and boreholes (especially gamma-ray well logs) to scale his geomagnetic polarity zones of the lower Buntsandstein continental facies of the Central Germany of latest Permian through Early Triassic. This resulted in an estimated duration of Induan Stage of about 1.8–2.2 Myr and duration for the Olenekian of about 3 Myr depending on the placements of the PTB, the Induan/Olenekian boundary and the top of the Olenekian within the lower Buntsandstein.

The cycle-scaled magnetostratigraphy of the continental Germanic Basin correlates well with the 5.1 Myr astronomical-calibrated time scale constructed by Li et al. (2016) using a 405-kyr long-eccentricity cycles tuning of spectral gamma-ray logs from the marine sections of Chaohu, Daxiakou, Guangdao and Meishan in South China. That study yielded durations for Induan and Olenekian stages of 2.0 and 3.1 Myr, respectively, and durations of 1.4, 0.6, 1.7 and 1.4 Myr for the Griesbachian, Dienerian, Smithian and Spathian substages, respectively. This estimated duration of 1.4 Myr for the Griesbachian substages based on 405 kyr tuning is also consistent with a duration of 1.6 Myr estimated from the Carnic Alps in Austria based on the ~ 100 kyr counting by Rampino et al. (2000). A similar cyclostratigraphy-derived duration of 1.7 ± 0.1 Myr for the Induan Stage was obtained from the conodont-dated distal Montney Formation of British Columbia that yielded a full suite of long-eccentricity, short-eccentricity, obliquity and precession cycles (Shen et al., 2017).

One contributing reason why the earlier studies by Guo et al. (2008) and Wu et al. (2012) had interpreted a short duration of only ~ 1.1 Myr for the Induan stage is because they assumed a fairly constant sedimentation accumulation rate for the spectral analysis of the entire section. However, the sedimentation accumulation rate appears to significantly change from the lower Yinkeng Formation (Griesbachian part) with thin mud/claystone interbedded with limestones into the middle Yinkeng Formation (Dienerian part) with the increasing thickness of mudstone interbedded with limestones. They had also assumed that the predominant cycles of ~ 0.8 m

are ca. 20-kyr precession cycles for the whole series; however, these predominant ~ 0.8 m cycles should be the ca. 33-kyr obliquity cycles from the middle Griesbachian to the end of Dienerian (10–74 m interval in Chaohu section) according to the ratio of the wavelengths of $\sim 10:2.3:0.9:0.5$ that is similar with the ratios of Milankovitch cycles of 405:100:33:20.

Therefore, based on an anchoring age of the U-Pb date of 251.9 Ma for the PTB (Burgess et al., 2014), an absolute ATS for the Early Triassic spanning 5.1 Myr from 251.9 to 246.8 Ma has been constructed based on the composite marine sections of Chaohu, Daxiakou, Guangdao and Meishan in South China (Li et al., 2016) (Fig. 4A). The calculated Induan/Olenekian boundary (I/OB) and Olenekian/Anisian boundary (O/AB) ages are 249.9 and 246.8 Ma from this ATS. The astronomical-calibrated O/AB age of 246.8 Ma is slightly younger than the U-Pb dates for the FAD of the proposed base-Anisian marker conodont *Chiosella timorensis* of 247.28 ± 0.12 Ma at the Guandao section (Lehrmann et al., 2015) and an interpreted 247.31 ± 0.06 Ma at the Monggan/Wantou section (Ovtcharova et al., 2015; although they recognized anomalies in the succession of U-Pb dates in the suite of ash beds). Therefore, when combined with the ammonoid and magnetostratigraphy global correlation, the estimated age for Early/Middle Triassic boundary, which has yet to be assigned a formal GSSP definition, is placed at a rounded 247 Ma (Ogg et al., 2016).

The 5.1 Myr duration for the Early Triassic composite ATS could be assigned as the appropriate 405-kyr chrono-cycles of E622 to E609.4 (Fig. 4A).

3.2 The Middle Triassic

The Middle Triassic includes **Anisian** and **Ladinian** stages and spanned about 10 Myr from the Early/Middle Triassic boundary at ~ 247 Ma to the Middle/Late Triassic boundary at 237 Ma. There are many cyclostratigraphy studies for the Middle Triassic Latemar limestone from 1980s (Goldhammer et al., 1987, 1990; Hardie et al., 1997; Hinnov and Goldhammer, 1991; Kent et al., 2004; Maurer et al., 2004; Mundil et al., 2003; Preto et al., 2001, 2004; Zühlke et al., 2003; Zühlke, 2004) (Fig. 3).

The Latemar carbonate platform in the Dolomites of Northern Italy was formed in the western tropical Tethys Ocean. The exposed platform facies of laminated limestones, wackestone, packstone and grainstone has about 500 meter-scale cycles (Goldhammer et al., 1987) or 600–700 shallowing-upward cycles or microcycles (Preto et al., 2004; Zühlke, 2004). The

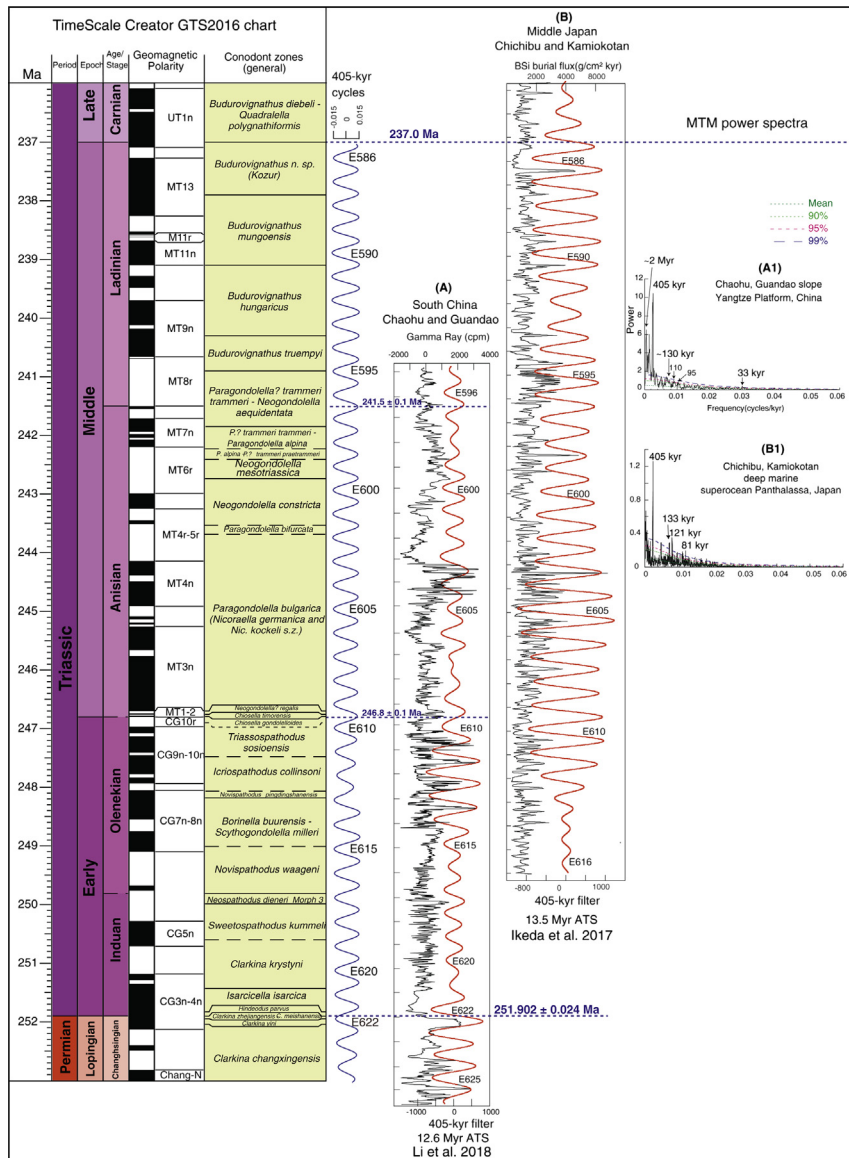


Figure 4 Our reanalysis and 405-kyr tuning of selected series for the Early-Middle Triassic ATS. Chronostratigraphy columns on the left were generated using TimeScale Creator 7.0 (engineering.purdue.edu/Stratigraphy/tscreator) with the GTS2016 integrated stratigraphy (Ogg et al., 2016). (A) Composite section of GR series (the original data from Li et al., 2018, using the GR residuals series after removing 10% weighted average) from Chaohu and Guandao section (South China) with 405 kyr filter output (red curve, passband: 0.00247 ± 0.00005 cycles/kyr). (B) BSi burial fluxes of chert series (the original data from Ikeda et al., 2017, using the BSi residuals series after removing 25% weighted average) with 405 kyr filter output (red curve, passband: 0.00247 ± 0.00005 cycles/kyr). (A1) and (B1) are 2π MTM power spectra of series in A and B, respectively.

estimated duration for the Latemar platform based on the orbital interpretations of these cycles is about 9–14 Myr (Goldhammer et al., 1990; Preto et al., 2004), which is ca. 4 times longer than its span indicated by the U-Pb zircon ages (Mundil et al., 1996, 2003; Brack et al., 1996, 2007). This “Middle Triassic Latemar controversy” mismatch between standard cyclostratigraphic analyses and the other stratigraphic interpretations was difficult to resolve. Kent et al. (2004) suggested a total duration of only \sim 1 Myr for the \sim 470 m thick Latemar carbonate platform in the Dolomites based on the lack of magnetic reversals, thereby implying a mean duration of \sim 1.7 kyr for the observed meter-scale cycles. A similar interpretation of high-frequency (1–2 kyr) meter-scale rhythmic beds in a basinal facies at the Rio Sacuz section of northern Italy was derived from the magnetostratigraphy and cyclostratigraphy of magnetic susceptibility proxies (Spahn et al., 2013). In this case, the total duration of the Latemar platform deposition, coupled with its uncertain biostratigraphic age span, is inadequate for calibrating the geological time scale.

In contrast, the Guandao marine section in the Guizhou Province of South China is an important reference section for integrated Anisian stratigraphy (Lehrmann et al., 2015). Li et al. (2018) resolved long-eccentricity cycles in over 300 m of these marine slope deposits of pelagic micrite-rich limestones with some carbonate packstone–grainstone turbidites and debris flow breccia beds. The analyses were based on 2061 magnetic susceptibility data points and 1071 spectral gamma-ray measurements at 5–20 cm sample intervals for a \sim 260 m series after removing the redeposited breccia beds. The predominant \sim 23 m cycles were assumed to be the stable 405-kyr long-eccentricity cycle based on the biostratigraphy and magnetostratigraphy constraints (Lehrmann et al., 2015), and tuning to this 405-kyr period produced a ca. 6 Myr ATS for all the Anisian conodont and magnetic polarity zones. The Anisian has a 5.3 Myr duration at this Guandao reference section; therefore, based on the 246.8 Ma age for the Olenekian/Anisian boundary based on the Early Triassic ATS from Chaohu and Daxiakou sections of South China, then the Anisian/Ladinian boundary is at 241.5 Ma (Li et al., 2016) (Fig. 4A). We reanalyzed the \sim 11 Myr composite GR series from South China marine sections spanning the entire Early Triassic and Anisian (Fig. 4A1, Table 1).

Volcanic ash beds in the Buchenstein Formation at Passo Feudo and Seceda in the Dolomites of Italy provides the U-Pb CA-ID-TIMS dates that bracket the Anisian/Ladinian boundary to be between

Table 1 Reanalysis of Selected Early-Middle Triassic Reference Sections Using Standardized Tuning to 405-kyr Long-Eccentricity Cycle and MTM Power-Spectra Analysis. Span (Myr) and Age Limits (Ma) are Based on the Interpreted Tuning Results

Location	Geologic-age	Data source	Proxy	Span (Myr)	Significant spectral cycles (kyr)		Assigned E-cycles	Age limits (Ma)
					E: 405 (tuned)	e: 130, 110, 95 O: 33		
Chaochu and Guandao (South China)	Uppermost Lopingian– lowest Ladinian	Li et al. (2018)	Gamma Ray (GR)	~ 12.6	E: 405 (tuned)	e: 130, 110, 95 O: 33	E626–E595	253.4–240.8
Inuyama, Japan	Lower Olenekian– basal Carnian	Ikeda et al. (2017)	Biologic silica flux	13.5	405	e: 131, 121, 81	E616–E583	249.5–236

241.705 ± 0.045 Ma and 240.576 ± 0.042 Ma; for an estimate on the GSSP Anisian/Ladinian boundary age of $241.43 \pm 0.15/0.17/0.31$ Ma. A boundary age of $241.464 \pm 0.064/0.097/0.28$ Ma was achieved by integrating high-resolution cyclostratigraphy (Wotzlaw et al., 2018), which is identical to the 241.5 Ma based on the ATS by Li et al. (2018).

The middle Triassic bedded chert sequence in the Inuyama area of central Japan consists of centimeter-scale rhythmic alternations of chert and shale beds with rich radiolarian fossils that is considered to have been deposited in a pelagic deep-sea environment (Ikeda et al., 2010). The 720 chert–shale couplets with an average 21 mm thickness recognized in the 33-m bedded chert succession appear to be productivity oscillations induced by the ~ 20 kyr precession cycle, and the bundles of about 20 chert–shale couplets represent modulation by the 405-kyr long-eccentricity cycle. However, that initial deep-sea 15 Myr-long floating ATS (Ikeda et al., 2010) had only limited biostratigraphy and lacked any magnetostratigraphy or isotopic dates. Therefore, Ikeda and Tada (2014) extended their work to compile 3346 chert–shale couplets through a 110-m thick deep sea bedded chert sequence in the Inuyama area that spans the Lower Triassic to Lower Jurassic and applied 405 kyr tuning. This ~ 70 Myr long ATS was anchored at the end-Triassic radiolarian extinction level at chert bed-number 2525 as 201.4 ± 0.2 Ma (Fig. 4B). Ikeda et al. (2017) presented the biogenic silica flux (BSi) series from radiolarian chert. We collected the BSi data for this ~ 70 Myr-long record from this author and performed the spectral analysis for the Early-Middle Triassic part (Fig. 4B, Table 1). Combined with radiolarian biostratigraphy events and U-Pb dates, Ikeda and Tada (2014) projected an age of 235.2 ± 0.9 Ma for a radiolarian-based Ladinian/Carnian boundary, but the lack of radiolarian calibration to Middle Triassic stages precludes obtaining accurate durations for the Anisian and Ladinian stages based on this deep sea bedded chert ATS (Fig. 4B). But when combining the estimated 235.2 ± 0.9 Ma for the Ladinian/Carnian boundary by Ikeda and Tada (2014) with the 241.5 Ma base-Ladinian age from Guandao ATS, then estimated duration for the Ladinian stage from these ATS scales is about 6.3 ± 0.9 Myr. However, in contrast to the radiolarian-based placement in the deep-sea cherts, Mietto et al. (2012) reported a U-Pb zircon date of 237.77 ± 0.14 Ma for an ash layer near the top of the Ladinian Stage from the Rio Nigra section, therefore suggested an older age of ~ 237 Ma for the Ladinian/Carnian boundary, therefore implying that the Ladinian Stage spans only 4.5 Myr.

In summary, the 5.3 Myr duration for the Anisian stage based on the ATS corresponds to the 405-kyr chrono-cycles from E609.4 (at 246.8 Ma) to E596 (at 241.5 Ma). The 11.6 Myr duration for the entire Middle Triassic from merging the south China and central Japan ATS appears to correspond to the 405-kyr chrono-cycles from E608.5 to E581 (Fig. 4, Table 1). However, for the Ladinian and Carnian stages of middle Triassic, more cyclostratigraphy studies is crucial and need to be developed and correlated and integrated with biostratigraphy, chemostratigraphy, magnetostratigraphy and radioisotopic dating to verify of the main 405-kyr tuned ATS.

3.3 The Late Triassic

The Late Triassic includes **Carnian**, **Norian** and **Rhaetian** stages, and spans about 36 Myr from \sim 237 Ma at Middle/Late Triassic boundary to 201.4 Ma at Triassic/Jurassic boundary. There are about 10 cyclostratigraphic studies for the Late Triassic published in the past three decades (Balog et al., 1997; Clemmanson et al., 1998; Cozzi et al., 2005; Hüsing et al., 2011; Ikeda and Tada, 2014; Ikeda et al., 2017; Kemp and Coe, 2007; Kent et al., 2017; Li et al., 2017; Olsen and Kent, 1996; 1999; Olsen et al., 2011; Preto and Hinnov, 2003; Vollmer et al., 2008; Zhang et al., 2015) (Fig. 3).

The Carnian Stage does not yet have a continuous cyclostratigraphy in a non-deep-sea chert facies. Zhang et al. (2015) analyzed the GR series from South China carbonate-rich facies with a transition to clastic-rich facies \sim 2.4 Myr cycle-calibrated magnetostratigraphy that spans the upper part of the Julian substage and lower part of the Tuvalian substage of the Carnian Stage (Fig. 5E).

A superb cyclostratigraphy study of terrestrial strata was enabled by a \sim 3500-m thick succession in the Newark Basin derived from 7 overlapping boreholes that cores a total of 6770 m. This unparalleled continuous record spans the Late Carnian to Early Hettangian stages (Olsen and Kent, 1996; Olsen et al., 2011; Kent et al., 2017). The succession in the lacustrine to fluvial facies is characterized by 3–6 m thick cycles that correspond to lake level variations responding to \sim 20 kyr precession periodicity in relative monsoonal rainfall. These basic cycles are grouped into \sim 12–18 m and \sim 60 m bundles that represent strongly modulation by \sim 100-kyr short and 405-kyr long-eccentricity cycles, respectively. This \sim 3500 m composite depth rank series presents about 22 Myr duration for Late Triassic (Olsen and Kent, 1996). We restudied the composited depth rank series (relative

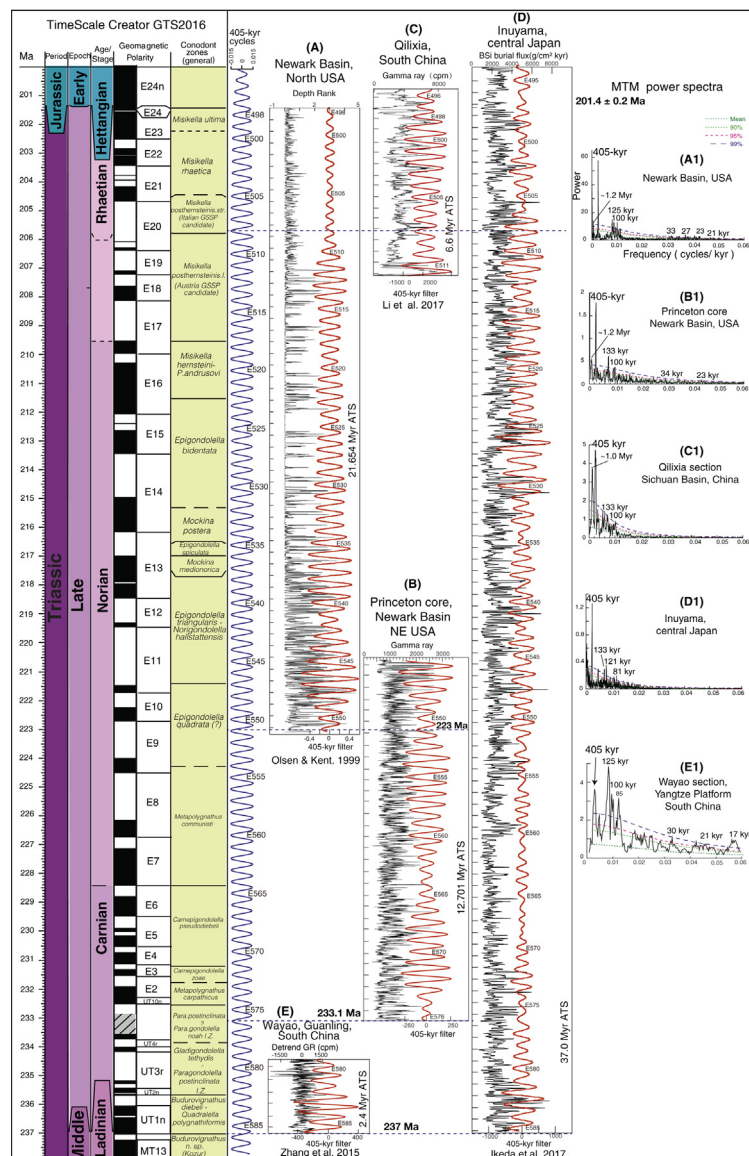


Figure 5 Our restudy and 405-kyr tuning of selected series for the Late Triassic ATS. Chronostratigraphy columns on the left were generated using TimeScale Creator 7.0 (engineering.purdue.edu/Stratigraphy/tscreator) with the GTS2016 integrated stratigraphy (Ogg et al., 2016). (A) The composite section depth rank series (the original data compiled by Olsen and Kent (1999) was downloaded from <https://www.idealocolumbia.edu/~polson/nbcn/data.html>, and retuned the composite depth rank residuals series using 405-kyr period in this study) from the Newark Basin (USA).

lake-depth or exposure intensity by Olsen and Kent, 1996) to recognize and tune the 53 predominant ~ 66 m wavelength cycles (405-kyr) in a large portion of their record. We constructed a ~ 21.65 Myr-long ATS based on tuning these ~ 66 m cycles to the 405-kyr long-eccentricity period (Fig. 5A, Table 2). In addition to this depth-rank proxy, we also analyzed the GR data from the Princeton drilled core in that Newark Basin set. A ~ 12.7 Myr-long ATS has been constructed based on the recognition of 31 predominant ~ 40 m cycles that were tuned to the 405-kyr long-eccentricity period (Fig. 5B, Table 2). According to the correlation provided by Kent et al. (2017; their Fig. 1), the 294 m level in the Princeton core could correlate with the base of composite depth-rank series at 223 Ma or chrono-cycle E551; thereby projecting the base of the Princeton GR ATS at 233.1 Ma or chrono-cycle E576 (Fig. 5B).

Applying the ATS to obtain cycle-durations of Late Triassic stages is hindered by their lack of standard GSSP definitions. Olsen et al. (2011) used their astronomically tuned geomagnetic polarity timescale (called Newark-Hartford APTS) to estimate approximate durations of $\sim 7 \pm 4$ Myr duration for the recovered portion of the Carnian Stage, a 6.2 Myr or 9.7 Myr for the Rhaetian Stage (depending whether a short or long option was used for its definition) and a 17.6–20.1 Myr duration for the Norian Stage depending upon the selected Rhaetian option. The main Newark lacustrine succession is capped by the massive basalt flows of the Central Atlantic Magmatic Province (CAMP) large igneous event, which are considered to be a major contributor to the end-Triassic global extinctions, and the base of the Jurassic corresponds to the first appearance of *Psiloceras spelae* ammonite. These have been dated by U-Pb methods, thereby enabling an absolute age scale for this Late Triassic ATS. The Triassic/Jurassic boundary is dated as 201.36 ± 0.14 Ma from bracketing ash beds on the ammonite occurrence in Peru by Wotzlaw et al. (2014; revising

(B) GR series of the Princeton core of the Newark Basin (USA) (we downloaded the original data from <https://www.ldeo.columbia.edu/~polson/nbcprince.core.html>, after removing some spikes to tune it to 405-kyr period). (C) GR series of the Qilixia Section from Sichuan Basin (South China) (the original data from Li et al., 2017). (D) BSi burial fluxes of chert series (data from Ikeda et al. (2017), the BSi residuals series after removing 25% weighted average). (E) GR series of the Wayao composite section (South China) (the original data from Zhang et al., 2015). All the 405-kyr filter output (red curve, passband: 0.00247 ± 0.0003 – 0.0008 cycles/kyr). A1-E1 are 2π MTM power spectrum of A-E series.

Table 2 Reanalysis of Selected Late Triassic Reference Sections Using Standardized Tuning to 405-kyr Long-Eccentricity Cycle and MTM Power-Spectra Analysis. Span (Myr) and Age Limits (Ma) are Based on the Interpreted Tuning Results

Location	Geologic-age	Data source	Proxy	Span (Myr)	Significant spectral cycles (kyr)	Assigned E-cycles	Age limits (Ma)
Composite core, Newark Basin (North USA)	Low Norian—uppermost Rhaetia	Oslen & Kent (1999), https://www.ldeo.columbia.edu/~polson/nbcp/data.html	Depth rank series	21.65	E: 405 (tuned) e: 125, 100 O: 33, 27 P: 23, 21	E551-E498	223.1–201.4
Princeton core, Newark Basin (North USA)	Middle Carnian—middle Norian	https://www.ldeo.columbia.edu/~polson/nbcp/prince.core.html	Gamma Ray (GR)	12.7	405 e: 133, 100 O: 34 P: 23	E576-E545	233.1–220.6
Qilixia section, Sichuan Basin (China)	Upper Norian—Lowermost Hettangian	Li et al. (2017)	Gamma Ray	6.4	405 e: 133, 100	E512-E496	207.2–200.8
Gayao, Guanling (South China)	Lower Carnian	Zhang et al. (2015)	Gamma Ray	2.4	405 e: 125, 100, 85 O: 30 P: 21, 17	E586-E579	234.6–237
Inuyama, Japan	Basal Carnian-lower Hettangian	Ikeda et al. (2017)	Biogenic silica flux	37.0	405 e: 131, 121, 81	E585-E494	237–200

the previous 201.3 ± 0.18 Ma by [Schoene et al., 2010](#)), and the basalts at the top of the Newark ATS have a suggested age of 201.4 Ma ([Sha et al., 2015](#)).

Applying the Newark-Harford APTS to the magnetostratigraphy correlation from the Tethyan marine sections of Pizzo Mondello (Italy) ([Muttoni et al., 2004](#)) and Silicka Brezova (Slovakia) ([Channell et al., 2003](#)), combined with conodont biostratigraphy ([Mazza and Rigo, 2012](#)) and a U-Pb date of 230.91 ± 0.33 Ma within the uppermost Carnian at the Pignola 2 marine section in Italy ([Furin et al., 2006](#)), [Kent et al. \(2017\)](#) estimated an age of about 227 Ma for the Carnian/Norian boundary and 205.5 Ma for the Norian/Rhaetian boundary. Therefore, including the base-Carnian date of 237 Ma ([Mietto et al., 2012](#)), then the durations of Carnian, Norian and Rhaetian (short-option) could be assigned as 10, 21.5 and 4.1 Myr, respectively based on the Newark-Hartford APTS. In contrast, based on radiolarians in their deep-sea chert-derived 70-Myr-long Inuyama-ATS, [Ikeda and Tada \(2014\)](#) proposed stage boundary ages of 235.2 ± 0.9 , 225.0 ± 1.1 and 208.5 ± 0.3 Ma for the Ladinian/Carnian, Carnian/Norian and Norian/Rhaetian boundaries, respectively; implying durations for Carnian, Norian and Rhaetian of 10.2, 16.5 and 7.1 Myr, respectively. [Hüsing et al. \(2011\)](#) also suggested a cycle-calibrated magnetostratigraphy that implied both a Long-Norian (~ 17 Myr) and a Long Rhaetian (~ 9 Myr), which is consistent with the Inuyama-ATS model. The GTS2016 ([Ogg et al., 2016](#)) assigned ages of 237 and 228.5 Ma for the Ladinian/Carnian and Carnian/Norian boundaries, and either 209.5 or 205.7 Ma for the Norian/Rhaetian boundary age based on the Austrian GSSP candidate (long-Rhaetian option) and the Italian GSSP candidate (short-Rhaetian option). It remains an embarrassment that we have a rather well-developed ATS for the ages of the entire Late Triassic magnetic polarity time scale, dinosaur evolution, atmospheric carbon dioxide history ([Schaller et al., 2015](#)) and other events; but have not yet decided on the definitions for the Norian and Rhaetian stages or their potential substages.

If the “short” Rhaetian option is used, which is based on a more restricted taxonomic definition for the basal-Rhaetian conodont marker, then the current best estimate age for the resulting Norian/Rhaetian boundary would be 205.50 ± 0.35 Ma based on bracketing U-Pb dates of 205.70 ± 0.15 and 205.30 ± 0.14 Ma ([Wotzlaw et al., 2014](#)) combined with the magnetostratigraphic (reversed-polarity Chron E20r.2r) cyclostratigraphy correlation from Newark APTS to a potential Norian/Rhaetian boundary candidate GSSP section at Pignola-Abriola in southern Italy ([Maron et al., 2015; Kent et al., 2017](#)). The combined cyclo-magnetic

ATS can also be applied to non-fluvial terrestrial deposits (e.g., Xujiahe and Qilixia sections) in Sichuan, China (Li et al., 2017a), and demonstrates a common negative carbon isotope excursion in organic matter (Li et al., 2017b,c). This short version of the Rhaetian spans 4.3 Myr in the ATS (Fig. 5AC).

Based on the Triassic-Jurassic boundary age of 201.4 Ma, the \sim 21.65 Myr-long ATS from Newark Basin could be assigned to the 405-kyr chrono-cycles from E 551 to E498. Even though the Inuyama-ATS could provide a 35.6 Myr scale for the Late Triassic spanning potentially 405-kyr chrono-cycles from E 585 to E497 (Fig. 5D), it does not yet have potential use for a reference standard due to lack of a more globally useful biostratigraphy, magnetostratigraphy or isotopic dating constraints. In contrast, when combining with the 405 kyr tuned GR series in this study from the Princeton drilled core, the Newark Basin provides nearly a 32 Myr-long ATS that could be assigned to the 405-kyr chrono-cycles from E576 to E498 (Fig. 5AB). This ATS with its magnetic chron and other calibrations could serve as a standard reference for the international geological time scale.

4. THE CURRENT STATUS OF THE JURASSIC ATS

The Jurassic Period begins with the lowest occurrence of ammonite *P. spelae* after the end-Triassic extinction is U-Pb dated as 201.4 ± 0.17 Ma (Wotzlaw et al., 2014). The top of Jurassic (Jurassic/Cretaceous boundary) has not been defined, but the candidates currently include the base of micro-fossil *Calpionella alpina* or the base of magnetic polarity Chron M18r at 145.5 Ma in GTS2012 (Ogg et al., 2012a; 2016). The bases of the 11 international Jurassic stages as assigned at GSSPs or at candidate definitions are at levels corresponding to the lowest occurrences of ammonoid taxa. Over 30 cyclostratigraphic studies have been published for the Jurassic in the past three decades (Fig. 6).

4.1 The Early Jurassic

The Early Jurassic includes **Hettangian**, **Sinemurian**, **Pliensbachian** and **Toarcian** stages and spans about 27 Myr from the Triassic/Jurassic boundary at 201.4 Ma to the Early/Middle Jurassic boundary at 174.2 Ma. Nearly 20 Early Jurassic cyclostratigraphic studies have been published over the past twenty years (Boulila et al., 2014; Hinnov and

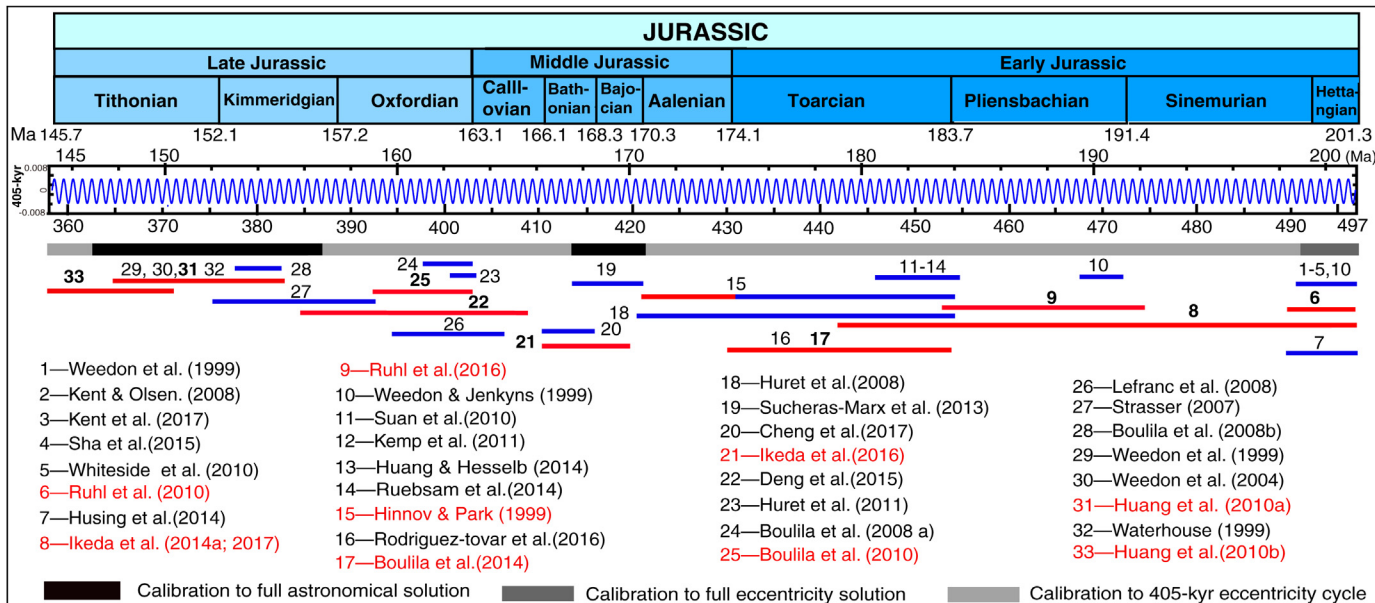


Figure 6 Stratigraphic coverage of the Jurassic ATS and 405-kyr metronome. Intervals with red lines (gray in print version) indicate the collected data coverage subjected to a 405-kyr tuning to compile the ATS in this study, and those with blue lines (dark gray in print version) indicate additional supporting cyclostratigraphy studies.

Park, 1999; Huang and Hesselbo, 2014; Hüsing et al., 2014; Ikeda and Hori, 2014; Ikeda et al., 2017; Kemp et al., 2011; Kent and Olsen, 2008; Kent et al., 2017; Rodriguez-tovar et al., 2016; Ruebsam et al., 2014; Ruhl et al., 2010; 2016; Sha et al., 2015; Suan et al., 2010; Weedon et al., 1999; Weedon and Jenkyns, 1999; Whiteside et al., 2010). Milankovitch signals of precession, obliquity and eccentricity have been recognized from outcrop sections in Britain and Southern Alps (Weedon et al., 1999; Hinnov and Park, 1999) (Fig. 6).

The Hettangian Stage has a duration of ca. 1.8 Myr according to the cyclostratigraphy at the St Audrie's Bay and East Quantoxhead (UK) outcrop section of the Bristol Channel Basin (Ruhl et al., 2010) and its correlation with the astronomically calibrated magnetostratigraphy sequence from the Hartford Basin (USA) of Kent and Olsen (2008). At the St Audrie's Bay, the 120 m thick succession of black-shale and limestone display 3.5–6 m thick cycles in $\delta^{13}\text{C}_{\text{org}}$, TOC, CaCO_3 and magnetic susceptibility data that were interpreted as \sim 100-kyr short-eccentricity cycles (Ruhl et al., 2010). We applied 405-kyr long-eccentricity cycle tuning for the $\delta^{13}\text{C}_{\text{org}}$ series based on the recognition of \sim 4.5 m (\sim 100 kyr) and \sim 16 m (405 kyr) cycles to construct a 3.55-Myr-long ATS (Fig. 7A, Table 3). The estimate duration of 1.97 Myr for the Hettangian Stage implies that the Hettangian/Sinemurian boundary age is 199.43 Ma (Fig. 7A), which is the same as the 2 Myr duration used in GTS2012 (Ogg et al., 2012a). Kent and Olsen (2008) constructed a 2.4 Myr-long APTS from the 2500 m succession in the Hartford Basin and estimated the duration for Hettangian Stage was also about 1.9 Myr; and, relative to the 201.4 Ma age for the Triassic/Jurassic boundary, this implied an age of 199.5 Ma for the Hettangian/Sinemurian boundary (Kent et al., 2017). Sha et al. (2015) obtained a similar result from the 300-m thick fluvial-lacustrine sequences in the Badaowan Formation of the Junggar Basin (China) based on the 405-kyr long-eccentricity correlation between the Newark–Hartford basins (USA), the Bristol Channel Basin (UK) and the Pucara Basin (Peru) and La2010d 405-kyr eccentricity theory curve.

Weedon and Jenkyns (1999) estimated a minimum duration of 4.82 Myr for the Pliensbachian Stage based on the cycle counting for the *T. ibex* (0.34 Myr) and *U. jamesoni* (1.42 Myr) ammonite zones from the assumed precession cycles of the light to dark marl bedding couplets sequence in

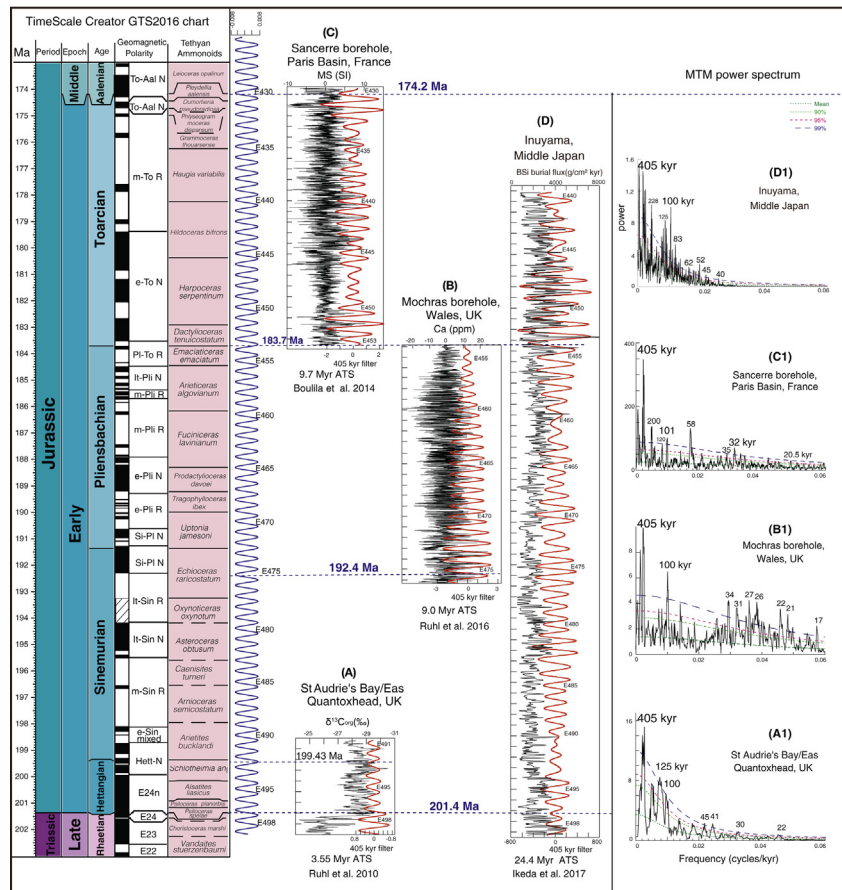


Figure 7 Our restudy and 405-kyr tuning of selected series for the Early Jurassic ATS. Chronostratigraphy columns on the left were generated using TimeScale Creator 7.0 (engineering.purdue.edu/Stratigraphy/tscreator) with the GTS2016 integrated stratigraphy (Ogg et al., 2016). (A) $\delta^{13}\text{C}_{\text{org}}$ series of the St Audrie's Bay (UK) (the original data from Ruhl et al. (2010), we retuned the $\delta^{13}\text{C}_{\text{org}}$ residuals series (after removing 25% weighted average) using 405 kyr period). (B) Ca content series of the Mochras Farm (Llanbedr) Borehole (UK) (data from Ruhl et al., 2016). (C) BSI burial fluxes of cherts residuals series (data from Ikeda et al., 2017), after removing 25% weighted average. (D) MS residuals series (after removing 10% weighted average) of the Sancerre-Couy drill-core in the southern Paris Basin (data download from <https://doi.pangaea.de/10.1594/PANGAEA.821258>, Bouilla et al. (2014)). All the 405 kyr filter output (red curve, passband: 0.00247 ± 0.00003 – 0.00008 cycles/kyr). A1-D1 are 2π MTM power spectrum of A-D series.

Table 3 Reanalysis of Selected Early Jurassic Reference Sections Using Standardized Tuning to 405-kyr Long-Eccentricity Cycle and MTM Power-Spectra Analysis. Span (Myr) and Age Limits (Ma) are Based on the Interpreted Tuning Results

Location	Geologic-age	Data source	Proxy	Span (Myr)	Significant spectral cycles (kyr)	Assigned E-cycles	Age limits (Ma)
St. Audrie's Bay (UK)	Uppermost Rhaetian-lowest Sinemurian	Rohl et al. (2010, online Suppl.)	$\delta^{13}\text{C}_{\text{org}}$	3.55	E: 405 (tuned) e: 125, 100 O: 45, 41 , 30 P: 22	E499–E491	202.2–198.65
Mochras Borehole (UK)	Uppermost Sinemurian-end Pliensbachian	Rohl et al. (2016)	Ca-series	9	405 e: 100 O: 34, 31, 27, 26 P: 22, 21, 17	E476–E454	192.7–183.7
Sancerre-Couy Borehole, Paris Basin (France)	Base-Toarcian–basal Aalenian	Boulila et al. (2014)	Magnetic susceptibility	9.7	405 e: 120, 101 O: 58 , 35, 32 P: 21	E454–E430	183.7–174.0
Inuyama, Japan	Upper Rhaetian–mid-Toarcian	Ikeda et al. (2017)	Biologic silica flux	24.4	405 e: 125, 100 , 83 O: 62, 52, 45, 40	E499–E440	202.3–177.9

the epicontinental sea of the Belemnite Marls (Dorset, southern England). Based on scaling the rate-of-change of marine Sr-isotope ratios, they projected minimum durations 2.86, 7.6 and 6.67 Myr for Hettangian, Sinemurian and Pliensbachian stages respectively. However, their estimated durations of the *T. ibex* (0.34 Myr) and *U. jamesoni* (1.42 Myr) ammonite zones from the Belemnite Marls is much shorter than the duration of ~ 1.8 and ~ 2.7 Myr for these two zones estimated from the more expanded records in the Mochras Borehole by Ruhl et al. (2016).

For the Pliensbachian Stage, Ruhl et al. (2016) present an over 9-Myr-long ATS based on the 405-kyr tuned Ca series from the marl and clayey limestone record of the Mochras Borehole drilled in the 1968–70 at Cardigan Bay Basin on the west coast of Wales. This ATS record includes well-defined ammonite zones, indicating durations of ~ 2.7 , ~ 1.8 , ~ 0.4 , ~ 2.4 and ~ 1.4 Myr for the *U. jamesoni*, *T. ibex*, *Psiloceras davoei*, *A. margaritatus* and *Psiloceras spinatum* zones, respectively (Fig. 7B). We applied 405 kyr tuning to their series to assign the interval to potential “E” cycles (Fig. 7B1, Table 3). Ruhl et al. (2016) obtained a ~ 8.7 Myr duration for the Pliensbachian stage and suggested that the Sinemurian/Pliensbachian boundary had an age of 192.5 ± 0.4 Ma relative to a radiometric date of 183.8 ± 0.4 Ma for the base of the Toarcian.

There is not yet a verified cyclostratigraphy scaling for the intervening Sinemurian Stage. However, the constraints of the Hettangian/Sinemurian boundary age of 199.5 Ma from the Newark-Hartford APTS proposed by Kent et al. (2017) and the 192.6 Ma age for the Sinemurian/Pliensbachian boundary age imply that the Sinemurian Stage spans ~ 7 Myr (Ruhl et al., 2016).

The Toarcian Stage astrochronology became a hot topic when trying to determine the rates and duration for the Early Toarcian Oceanic Anoxic Event (T-OAE). Depending on the interpretation of the dominant and superimposed cycles, the interpreted durations for the T-OAE and its associated negative carbon-isotope excursion (CIE) have ranged from 200 kyr to 1.0 Myr (Ait-Itto et al., 2018; Boulila et al., 2014; Huang and Hesselbo, 2014; Hüsing et al., 2014; Ikeda and Hori, 2014; Kemp et al., 2011; Martinez et al., 2017; Müller et al., 2017; Ruebsam et al., 2014; Ruhl et al., 2010; Suan et al., 2010). However, these cyclostratigraphy studies mainly focused on the brief T-OAE interval. The main current reference ATS for the entire Toarcian stage is from the gray marine marls in the Sancerre-Couy drill-core (194.55–360 m) in the southern Paris Basin that has a well-defined ammonite biostratigraphy. Boulila et al. (2014)

measured a high-resolution magnetic susceptibility data series for the Sancerre–Couy drill-core and interpreted ~ 8 m (405 kyr) and ~ 32 m (1.6 Myr) cycles characterized the entire Toarcian Stage. Based on the 405-kyr long-eccentricity cycle tuning, they estimated a ~ 300 to 500 kyr duration for the Toarcian CIE and a minimum duration of ~ 8.3 Myr for the Toarcian Stage. We reanalyzed this MS series and recognized 24 predominant ~ 8 m cycles (405-kyr) to construct a ~ 9.7 Myr-long ATS based on a similar 405-kyr tuning (Fig. 7C, Table 3). Our estimate duration for the Toarcian Stage is ~ 9.5 Myr, which is similar to 9.5 Myr duration assigned for this stage in GTS2016 (Ogg et al., 2016).

Toarcian cyclostratigraphy has also been studied in the Italian and French Alps. Hinnov and Park (1999) studied the rank series of the bedded basinal carbonate succession of the Colle di Sogno section in the Lombard Basin of the Southern Alps. Based on counting the obliquity cycles, they estimated a minimum duration of 11.37 ± 0.05 Myr for the combined Toarcian–Aalenian stages. Huret et al. (2008) restudied the rank series of the Aalenian part between 83–130 m from this Sogno section and estimated a duration of 3.85 Myr for the Aalenian Stage. Their duration for the Toarcian Stage from the Sogno Section of 7.52 Myr is significantly less than the 8.3 Myr duration estimated from the Sancerre core by Boulila et al. (2014).

On the broad scale for nearly the entire Triassic through Early Jurassic, Ikeda et al. (2017) constructed ~ 70 Myr-long BSi ATS from the deep-sea bedded-chert sequence exposed in the Inuyama area of the central Japan based on the 405-kyr long-eccentricity cycle tuning and anchored at 201.4 ± 0.2 Ma for the end Triassic radiolarian extinction event (Fig. 7D). Their super long ATS spans 249.5 Ma to ca. 177.9 Ma. Their proposed ATS age of 183.4 ± 0.5 Ma for their placement of the Pliensbachian/Toarcian boundary is similar to the 183.7 Ma assigned age in the GTS2016 (Ogg et al., 2016). Our analysis (Fig. 7D, Table 3) suggested that the Jurassic portion of this Inuyama series could be the 405-kyr chrono-cycles from E497 to E440. However, as with the Triassic, these cyclostratigraphy studies could not provide us an accurate time scale for the Early Jurassic there has been better calibration of the deep-sea stratigraphy.

The Hettangian Stage could be assigned to chrono-cycles from E497.3 to E493 based on the age of 201.4 Ma for the Triassic/Jurassic boundary and the 1.97 Myr duration from the 405 kyr tuned $\delta^{13}\text{C}_{\text{org}}$ series from

the Bristol Channel Basin (UK). Combining the ~ 9.3 Myr-long ATS for the Late Sinemurian and the entire Pliensbachian Stage from the 405 kyr tuned Ca series from the Mochras core (Ruhl et al., 2016) and the GTS2016 assigned age of 183.7 Ma for the base of the Toarcian (Ogg et al., 2016) implies a possible coverage of 405-kyr chrono-cycles from E476 to E454. The 9.5 Myr-long ATS for the Toarcian Stage could be assigned the chrono-cycles from E454 to E430.

4.2 The Middle Jurassic

The Middle Jurassic includes **Aalenian, Bajocian, Bathonian and Callovian stages** that spanned about 11 Myr from the Early/Middle Jurassic boundary at ~ 174 Ma to the Middle/Late Jurassic boundary at ~ 163 Ma. There are only a few cyclostratigraphic studies published for the Middle Jurassic over the past twenty years (Cheng et al., 2017; Hinnov and Park, 1999; Huret et al., 2008; Ikeda et al., 2016; Sucheras-Marx et al., 2013; Weedon et al., 1999) (Fig. 6).

The Aalenian Stage has been analyzed for cyclostratigraphy mainly using a lithostratigraphy rank series of the Sogno Section in the Lombardy Pre-Alps, Italy. Huret et al. (2008) reanalyzed the rank-series data collected by Hinnov and Park (1999) to propose a minimum duration of 3.85 Myr, and this result was incorporated as part of the calibration of the Aalenian time scale in GTS2012 (Ogg et al., 2012a). However, we re-analyzed this data in this study and derived a 4.44 Myr-long ATS based on the 405 kyr tuning the envelope of rank series (Fig. 8A, Table 4). The resulting estimated duration for the Aalenian stage of ~ 4 Myr is slightly longer than the 3.9 Myr duration assigned in the GTS2016, although that estimate had relatively high uncertainties of ± 1.0 to ± 1.4 Myr on the bounding stage boundaries (Ogg et al., 2016). Based on the projected age of 174.2 Ma for the Toarcian/Aalenian boundary, the 4 Myr Sogno ATS for the Aalenian stage could be assigned as the 405-kyr chrono-cycles from E430 to E420 (Fig. 8A).

Bajocian through Callovian chert abundances and color at the Torre De Busi and Corre Di Sogno sections in the Lombardian Basin (Northern Italy) was analyzed by Ikeda et al. (2016) to establish a ~ 4 Myr-long ATS. Their scale was based on the assumption that the observed cycles of 8, 16, 40 and 160 cm corresponded to ~ 20 , 40, 100 and 405 kyr cycles based on the biostratigraphic age constraints. We used their chert abundance series from Ikeda et al. (2016) supplementary data to construct a ~ 4.2 Myr-long ATS and based on tuning the predominant ~ 1.6 m thick

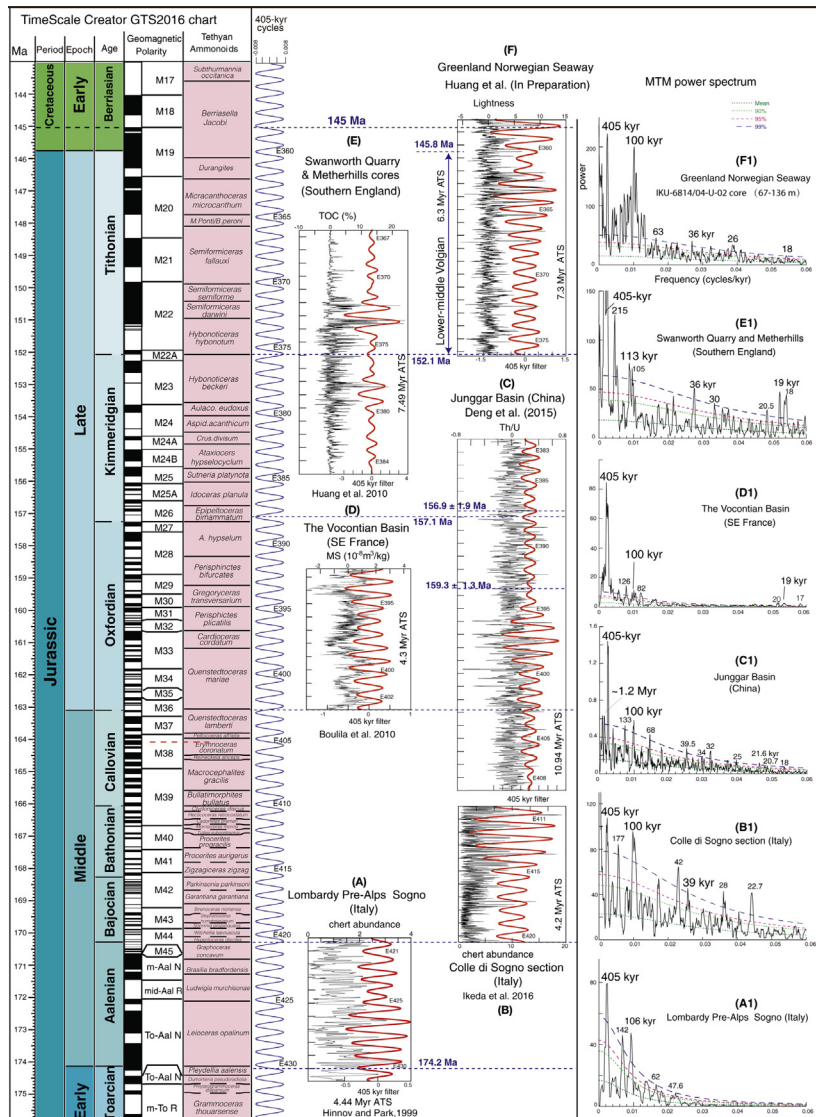


Figure 8 Our restudy and 405-kyr tuning of selected series for the Middle-Late Jurassic ATS. Chronostratigraphy columns on the left were generated using TimeScale Creator 7.0 (engineering.purdue.edu/Stratigraphy/tscreator) with the GTS2016 integrated stratigraphy (Ogg et al., 2016). (A) Chert abundance series (the original data from Hinnov and Park, 1999). (B) Chert abundance series of Chichibu and Kamiokotan areas (Japan) (the original data from Ikeda et al. (2016) supplementary data online at <https://doi.org/10.1016/j.palaeo.2016.06.009>). (C) Th/U residuals series (the original data from Deng et al., 2015, after removing 15% weighted average). (D) MS residuals series from the composited three Terres Noires sections of the Vocontian Basin

cycles to the 405-kyr long-eccentricity period (Fig. 8B, Table 4). This ~ 4 Myr-long Corre Di Sogno ATS which could be considered as the extension of the Toarcian-Aalenian Sogno ATS from the Lombardy Pre-Alps had been interpreted to span much of the Bajocian and Bathonian stages and could be assigned as the 405-kyr chrono-cycles from E420 to E410.

In contrast, a much longer duration for the lower Bajocian was estimated by Sucheras-Marx et al. (2013) based on a 169 m thick CaCO_3 wt% series from the Chaudon–Norante section of the French Subalpine Basin in France. They estimated a duration of 4.082 ± 0.144 Myr for the Early Bajocian based on the recognition of the 0.48–0.84, 0.98–1.43, 2.8–3.84 and 12–16 m cycles that assumed to correspond to precession, obliquity, short and long-eccentricity cycles. However, a 4.08 Myr duration for only the Early Bajocian is difficult to reconcile with the GTS2012 assigned duration of 2 Myr for the entire Bajocian stage without greatly shortening at least one other geologic stage within the Middle Jurassic through Early Cretaceous.

For the Bathonian Stage, Cheng et al. (2017) constructed a 2.09 Myr ATS based on the recognition of ~ 100 kyr cycles (~ 26 m) in the 557 m thick GR well log series of the drilled core from the marine carbonate Buqu Formation in the Qiangtang Basin (Tibet, China) and proposed a 2.09 Myr-long ATS for the Bathonian Stage. This result is compare closely to the 2.2 ± 1.3 Myr duration assigned in the GTS 2012 and 2016 that was partly constrained by radiometric dates from Pacific ODP Site 801 near the Bajocian/Bathonian biostratigraphic boundary (Ogg et al., 2012a; 2016). Due to the lack of consistent results for the Bajocian and Bathonian stage, and the lack of a calibrated ATS for the Callovian Stage, we could not compile the majority of the Middle Jurassic into the composite cyclo-chron figure.

(SE France) (the original data from Boulila et al., 2010, after removing 25% weighted average). (E) TOC residuals series (the original data from Huang et al., 2010, after removing 10% weighted average). (F) Lightness residuals series of the IKU-6814/04-U-02 core in the Greenland-Norwegian Seaway (the original data download from <http://doi.pangaea.de/10.1594/PANGAEA.141090> posted by Swientek (2004), after removing 15% weighted average). All the 405 kyr filter output (red curve, passband: 0.00247 ± 0.0003 – 0.0008 cycles/kyr). A1–F1 are 2π MTM power spectrum of A–F series.

Table 4 Reanalysis of Selected Middle-Late Jurassic Reference Sections Using Standardized Tuning to 405-kyr Long-Eccentricity Cycle and MTM Power-Spectra Analysis. Span (Myr) and Age Limits (Ma) are Based on the Interpreted Tuning Results

Location	Geologic-age	Data source	Proxy	Span (Myr)	Significant spectral cycles (kyr)	Assigned E-cycles	Age limits (Ma)
Lombardy Pre-Alps Sogno (Italy)	Uppermost Toarcian-Basal Bajocian	Hinnov & Park (1999)	Chert abundance	4.44	E: 405 (tuned) e: 142, 106 O: 62, 47.6	E431-E420	174.6–170.16
Colle di Sogno section (Italy)	Basal Bajocian-basal Callovian	Ikeda et al. (2016, online suppl.)	Chert abundance	4.2	405 e: 100 O: 42, 39 , 28 P: 22.7	E420.5-E410	170.3–166.1
Junggar Basin (China)	Lower Callovian-middle Kimmeridgian	Deng et al. (2015)	Th/U	10.9	405 e: 133, 100 O: 39.5 , 34, 32 P: 21.6 , 20.7, 18	E409-E382	165.6–154.7
Vocontian Basin (SE France)	Basal-upper Oxfordian	Boulila et al. (2010)	Magnetic susceptibility	4.3	405 e: 126,100 , 82 P: 20 , 19, 17	E403-E392.5	163.1–158.8
Swanworth Quarry & Metherhills cores (England)	Lower Kimmeridgian-upper Tithonian	Huang et al. (2010)	TOC (%)	7.49	405 e: 113 , 105 O: 36 , 30 P: 20.5, 19 , 18	E385-E366.5	155.74–148.25
Greenland Norwegian Seaway	Basal Tithonian-basal Berriasian	Huang et al. (preparation)	Lightness	7.3	405 e: 100 O: 36 , 26 P: 18	E376-E358	152.1–144.8

4.3 The Late Jurassic

The Late Jurassic includes **Oxfordian**, **Kimmeridgian** and **Tithonian stages** and spanned about 18 Myr from \sim 163 Ma at Middle/Late Jurassic boundary to \sim 145 Ma at Jurassic/Cretaceous boundary. There are nearly a dozen cyclostratigraphic papers have been published for the Late Jurassic over the past twenty years (Boulila et al., 2008a, b, 2010; Deng et al., 2015; Huang et al., 2010a,b; Strasser, 2007; Swientek, 2002; Waterhouse, 1999; Weedon et al., 1999, 2004) (Fig. 6).

An interval of lower Callovian through lower Kimmeridgian of Junggar Basin of northwest China was analyzed by Deng et al. (2015) to propose a \sim 10.9 Myr-long synthesized time scale. They used the Th/U series from an inner lacustrine succession that mainly consists of red mudstone-sandstone interbedded with gray shale, gypsum and volcanic ash beds. The geologic age assignments to the cyclostratigraphy were based on comparing to biostratigraphy, magnetostratigraphy and two SHRIMP U-Pb dates of 159.3 ± 1.3 Ma and 156.9 ± 1.9 Ma, thereby interpreting this series as spanning \sim 165.6 Ma (Early Callovian) to \sim 154.7 Ma (Early Kimmeridgian) and with projected ages of 161.5 Ma for the Callovian/Oxfordian boundary and 157.1 Ma for the Oxfordian/Kimmeridgian boundary. Their proposed Oxfordian/Kimmeridgian boundary age of 157.1 Ma is similar to the GTS2012 assigned age of 157.3 ± 1.0 Ma, but their estimated base-Oxfordian age is about 1.5 Myr younger. We reanalyzed this Th/U series and recognized 27 dominant \sim 50 m thick cycles to construct a 10.93 Myr-long ATS based on tuning these \sim 50 m cycles to the 405-kyr long-eccentricity period (Fig. 8C, Table 4). This 10.93 Myr-long Junggar lacustrine ATS could be assigned as 405-kyr chrono-cycles from E409 to E382 (Fig. 8C).

The cyclostratigraphic durations of Oxfordian ammonite zones are well constrained from the cyclic clayey and marly sediments of the Terres Noires Formation in the Vocontian Basin of southeast France and coeval deposits in the Paris Basin. Boulila et al. (2008a) collected 667 samples for the MS data measurement from the \sim 333-m thick outcrop in the Aspres-sur-Buëch section and measured the MS series from the EST342 drill-core in the eastern Paris Basin (France). Based on the recognition of clear visible \sim 55 and \sim 6 m cycles in the two series and assuming these cycles response to the 405-kyr long-eccentricity cycles and tuned these two MS series, they constructed an over 2 Myr-long ATS. Boulila et al. (2010) composited three Terres Noires sections and recognized 10 major

cycles that were assigned as 405-kyr long-eccentricity cycles to construct a ~ 4.3 Myr-long ATS for the Early-Middle Oxfordian stage (Fig. 8D). Even though their estimated duration for the entire Early-Middle Oxfordian of about 4.07 Myr from the 405 kyr tuned composite MS ATS, was similar with assigned duration of 3.8 ± 1.4 Myr in the GTS2004 (Gradstein et al., 2004), the relative durations of the component ammonite zones were significantly different. For example, they estimated a ~ 2.2 Myr duration for the *Q. mariae* ammonite zone in the Early Oxfordian stage, which was much longer than the 0.6 Myr duration assigned in GTS2004 based on applying equal ammonite subzonal durations (Gradstein et al., 2004), but was also shorter than the estimated duration of 2.7 Myr based on French borehole cyclostratigraphy by Lefranc et al. (2008). The composite Terres Noires ATS by Boulila et al. (2010) was used as the reference standard for the early portion of the Oxfordian time scale in GTS2012 (Ogg et al., 2012a). This interval could be assigned as the 405-kyr chrono-cycles from E403 to E392.5 (Fig. 8D, Table 4).

The Kimmeridgian cyclostratigraphy has been studied in both the Tethyan and Subboreal biogeographic realms. In the Tethyan realm, Strasser (2007) proposed a 3.2 Myr duration for the early Middle Oxfordian through earliest Kimmeridgian and $\sim 3.2\text{--}3.3$ Myr duration for the Kimmeridgian from the shallow carbonate platform of the Swiss and French Jura Mountains record based on the counting the small-scale sequences considering as ~ 100 -kyr short-eccentricity cycles. Boulila et al. (2008b) constructed a ~ 1.6 Myr ATS for the Early Kimmeridgian from the ~ 43 -m thick alternating marl-limestone succession of pelagic outcrop at La Méouge section of the Vocontian Basin (southeastern France) that shows high amplitude precession cycles and strongly 405-kyr long-eccentricity cycles.

In the Subboreal realm, Weedon et al. (2004) measured a 542-m succession for MS, PEF, total gamma-ray (GR) and total organic carbon (TOC) from a composite of three boreholes into the type Kimmeridge Clay Formation in Dorset (Southern England). Spectral analysis results showed long-wavelength cycles of 1.87–4.05 m; and they assumed these long cycles were ~ 38 kyr obliquity cycles to construct a 7.5 Myr-long ATS based on tuned the series using obliquity cycle. The estimate durations were 3.6 Myr (95 obliquity cycles) for the “early” Kimmeridgian Stage (from *Psiiloceras baylei* to *A. autissiodorensis* Subboreal ammonite zones) in Subboreal usage that is equal to the international Kimmeridgian Stage as defined by Tethyan ammonites, and 3.9 Myr (103 cycles) for the “late” Kimmeridgian

(from *Psiloceras elegans* to *V. fittoni* zones) in Subboreal usage that is equal to the early Tithonian Stage in international usage.

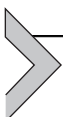
These initial outcrop-based Kimmeridgian Clay studies were enhanced by detailed borehole-based analyses. Huang et al. (2010a) analyzed the TOC series from the composite core section for the Kimmeridge Clay Formation and found hierarchy of cycles of ~ 1.6 , ~ 3.8 , ~ 9.1 and ~ 40 m wavelengths that corresponding to ~ 20 kyr precession, ~ 36 kyr obliquity, ~ 100 and 405-kyr short and long-eccentricity cycles respectively. They constructed a ~ 6.8 Myr ATS based on progressively tuning the TOC series to 405 kyr, ~ 100 and ~ 36 kyr cycles. However, we reanalyzed the TOC series and added two more possible 405 kyr cycles compared with the previous study to construct a 7.49 Myr-long ATS based on the 405 kyr cycle tuning (Fig. 8E, Table 4). The estimated duration for the “early” Kimmeridgian (except its lower *R. cymodoce* and *P. baylei* zones) and “late” Kimmeridgian are 3.64 Myr and 3.85 Myr, respectively, which is similar to the ~ 7.5 Myr ATS based only on 38 kyr obliquity tuning by Weedon et al. (2004). Assigning the base of the Subboreal *P. elegans* ammonite zone as the Kimmeridgian/Tithonian boundary using its assigned age of 152.1 Ma based on scaling Pacific marine magnetic anomalies (GTS2012; GTS2016), then the TOC ATS spans 155.74 and 148.25 Ma, respectively. This ~ 7.49 Myr-long Kimmeridge Clay ATS could be assigned as the 405-kyr chrono-cycles from E384.5 to E366.

An ATS for the combined Tithonian and Berriasian stages from cyclo-magnetostratigraphy studies in Argentina (Kietzmann et al., 2018 this volume) is briefly summarized in the next section on Early Cretaceous.

The Boreal Volgian Stage, which has a base that might be equivalent to the base of the Tethyan (international) Tithonian Stage, has been analyzed in boreholes from the Norwegian Sea. Huang et al. (2010b) analyzed the ~ 184 -m Lightness-data series from the core IKU-6814/04-U-02 that had been drilled in the Greenland-Norwegian Seaway (Swientek, 2002). The facies of laminated organic rich shales with in meter-scale intercalations of carbonate beds had been deposited in relatively deep water (Swientek, 2002). The power spectrum of this high-resolution lightness series (65–191 m) reveals sedimentary cycles with wavelengths at ~ 4 , ~ 1 , ~ 0.34 and ~ 0.2 m. We construct a ~ 13.66 Myr-long ATS based on the calibrating ~ 4 m cycles to the 405-kyr long-eccentricity cycles and estimated a 6.08 Myr duration for the combined Early and Middle Volgian substages (135–191 m). In this study, we reanalyzed the Lightness

series of the 8.39–191.29 m interval for the entire core record and recognized totally 63 cycles with ~2- to 5-m wavelength. A ~25.6 Myr-long high-resolution continuous ATS is based on tuning the ~2–5 m cycles to 405-kyr long-eccentricity cycles (Fig. 8F, Table 4). The resulting ~6.3 Myr duration for the combined Early and Middle Volgian substages (135–191 m) is close to the span of the Tithonian Stage if a lower Jurassic/Cretaceous boundary definition is used (Fig. 8F). This ~6.3 Myr-long Greenland-Norwegian ATS could be assigned as the 405-kyr chrono-cycles from E376 to E360 (Fig. 8F).

However, for the Jurassic, one or more cyclostratigraphy studies is crucial and need to be developed to cover the Sinemurian of the Early Jurassic, the most of Middle Jurassic includes **Aalenian**, **Bajocian**, **Bathonian** and **Callovian stages**. For the Late Jurassic, a duplicate study sections need to correlated and integrated with biostratigraphy, chemostratigraphy, magnetostratigraphy and radioisotopic dating to verify of the main 405-kyr tuned ATS for these three stages (**Oxfordian**, **Kimmeridgian** and **Tithonian stages**).



5. THE CURRENT STATUS OF THE CRETACEOUS ATS

5.1 The Early Cretaceous

The Early Cretaceous includes **Berriasian**, **Valanginian**, **Hauterivian**, **Barremian**, **Aptian** and **Albian stages** and spanned about 45 Myr from ~145 Ma at Jurassic/Cretaceous boundary to ~100 Ma at Early/Late Cretaceous boundary. There are about 16 cyclostratigraphic studies published for the Early Cretaceous over the past twenty years (Amadio et al., 2013; Charbonnier et al., 2013; Fiet, 2000; Fiet et al., 2001; Fiet and Gorin, 2000; Gale et al., 2011; Giraud et al., 1995; Grippo et al., 2004; Huang et al., 1993; Huang et al., 2010b,c; Liu et al., 2017; Martinez et al., 2012; 2013; 2015; Sprenger and ten Kate, 1993; Sprovieri et al., 2006) (Fig. 9).

The Berriasian Stage currently has a partial ATS that is mainly derived from magnetostratigraphy sections in Argentina (Kietzmann et al., 2015, and in press this volume). Sprenger and ten Kate (1993) analyzed the 77.5 m long CaCO₃ content series collected from the rhythmic hemipelagic limestone-marl sequence in the Caravaca region of southeast Spain and recognized ~30, ~6.67 and ~1 m cycles. They assigned the ~6.67 m cycles as ~100-kyr short-eccentricity cycle to tune this series,

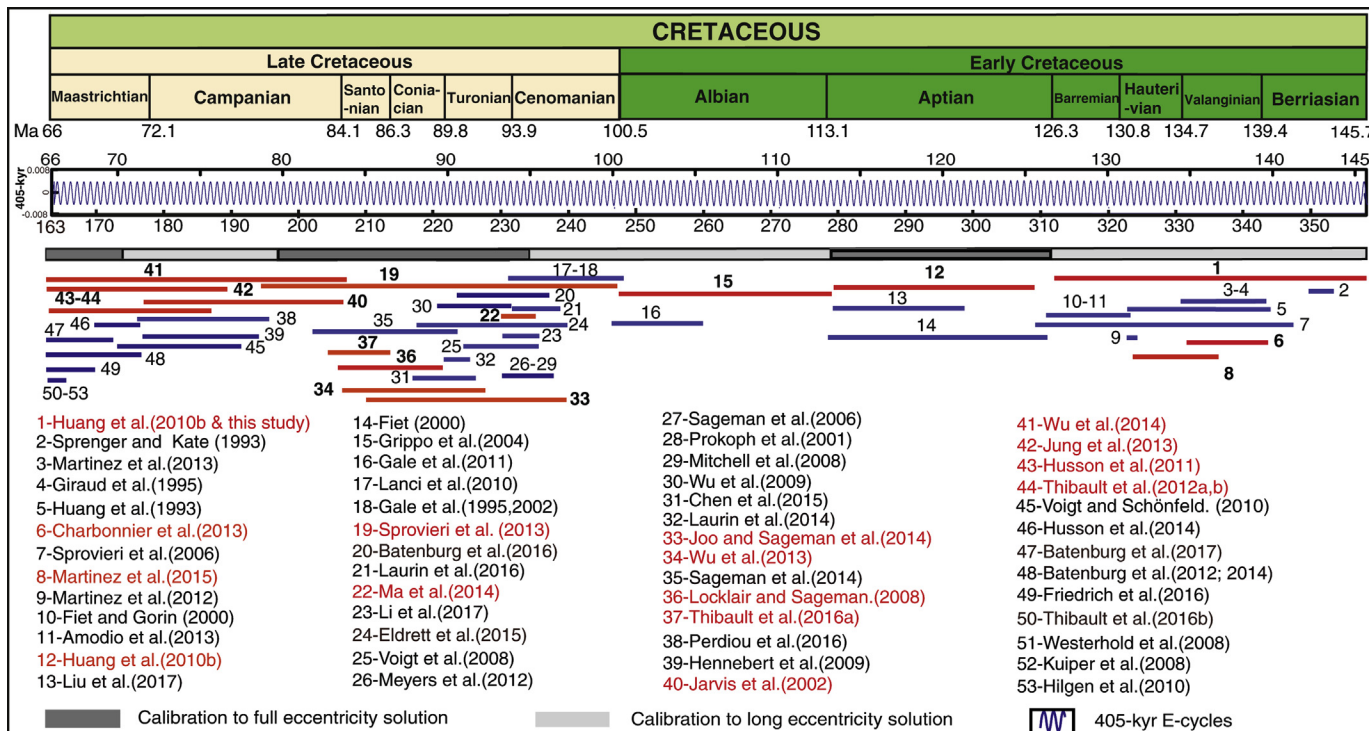


Figure 9 Stratigraphic coverage of the Cretaceous ATS and 405-kyr metronome. Intervals with red lines (gray in print version) indicate the collected data coverage subjected to a 405 kyr tuning to compile the ATS in this study, and those with blue lines (dark gray in print version) indicate additional supporting cyclostratigraphy studies.

and estimated a duration of 1.1–1.2 Myr for the *Calpionellopsis simplex* (D1) and *Calpionellopsis oblonga* (D2) subzones of upper Berriasian. A nearly complete Berriasian ATS was derived from alterations of marl and limestone in multiple sections of the Vaca Muerta Formation in the Neuquén Basin of Argentina (Kietzmann et al., 2015, and in press this volume). Even though the ammonite zonation of the Neuquén Basin is mainly endemic, the resolution of the complete suite of cycle-scaled magnetic polarity Chron M22r through Chron M15r enable a detailed correlation to the magnetic polarity time scale that has been calibrated to most of the Tethyan ammonite zones. The composite suite of sections spans the lowest Tithonian to nearly the top of the Berriasian. The bundling of the ca. 20- to 40-cm basic cycles is interpreted as long- and short-eccentricity modulation of precession cycles. They conclude that the Tithonian spanned a minimum of 5.67 Myr, and the Berriasian spans at least 5.27 Myr (Kietzmann et al., 2018 this volume).

The Valanginian Stage has been extensively analyzed in limestone-dominant to marl-dominant alternations in the Vocontian Basin of Southeastern France. Giraud et al. (1995) recognized 91 precession cycles and 137 obliquity cycles based on spectral analysis of the CaCO₃ content series, and proposed a duration of 7.04 Myr for the Valanginian Stage. However, Martinez et al. (2013) provides a shorter duration of 5.08 Myr for the Valanginian Stage based on the 405-kyr long-eccentricity cycle tuning the Gamma-Ray Spectrometry (GRS) series from the Vergol-Morénas, La Charce, Angles and Reynier sections with intercalibration between ammonite and calcareous nannofossil biozones and carbon-isotope stratigraphy in these well-defined biostratigraphy sections. Charbonnier et al. (2013) analyzed the 250-m thick high-resolution magnetic susceptibility data series from the hemipelagic marl-limestone alternations at the Orpierre section spanning from the Upper Berriasian to Valanginian. The prominent \sim 21, \sim 6.46, \sim 1.1–1.44 and \sim 0.71–1.02 m cycles could be correspond to 405-kyr, \sim 100 kyr eccentricity cycles, \sim 34 kyr obliquity and \sim 20 kyr precession cycles. A \sim 5.08 Myr-long high-resolution ATS was been constructed based on tuning the \sim 21 m cycles to the 405-kyr long-eccentricity cycles, and they proposed a 4.695 Myr duration for the Valanginian stage, which was used in GTS2016 (Ogg et al., 2016) rather than 5.5 Myr duration assigned in GTS2012 (Ogg et al., 2012b).

The Hauterivian and Barremian stages in the Vocontian Basin has similar alternations of limestone and marl as in the underlying Valanginian.

[Martinez et al. \(2015\)](#) analyzed the GRS series of the La Chare–Pommerol (240 m) sections spanning Upper Valanginian to Hauterivian, plus compared to the Río Argos (160 m) sections in southern Spain. They derived a 5.93 ± 0.41 Myr duration for the Hauterivian stage based on the identification of more than fourteen $\sim 11\text{--}28$ m wavelengths cycles that were assumed to correspond to the 405 kyr eccentricity. We combined the three sections of Reynier, La Chare–Pommerol and Río Argos as a composite 442.93 m long GRS series from the Late Berriasian to Early Barremian stages. This enabled a ~ 12.56 Myr-long ATS based on the recognition thirty-one ~ 15 m cycles tuned to the 405-kyr long-eccentricity cycles ([Fig. 10A, Table 5](#)). The estimate durations for Valanginian and Hauterivian stages are ~ 5.3 and 5.93 Myr, respectively. When we anchored the 12.3 m level at the Reynier section to a 139.4 Ma age for the Berriasian/Valanginian boundary, then the top of this ATS series reaches 127.4 Ma. In this case, the ~ 12.56 Myr-long ATS could be assigned as the 405-kyr chrono-cycles from E345 to E314 ([Fig. 10A](#)).

The Valanginian through Barremian cyclic sediments are also characteristic of the deep-sea successions in the Central Atlantic and uplifted Tethyan sections in Italy. [Huang et al. \(1993\)](#) estimated the minimum durations of 5.9 and 5.3 Myr for the Valanginian and Hauterivian stages based on comparing the cyclic sequences from the Central Atlantic and the Vocontian Basin (Southeast France). [Sprovieri et al. \(2006\)](#) analyzed the composite high-resolution pelagic bulk carbonate stable isotope record in three well-exposed sequences sections (Chiaserna Monte Acuto, Bosso, and Gorgo a Cerbara) in central Italy. They constructed a ~ 19 Myr-long ATS and estimated durations of ~ 6.9 , ~ 3.5 and ~ 4.4 Myr for the Valanginian, Hauterivian and Barremian stages, respectively, and proposed that the base of a positive carbon isotope excursion was at ~ 136.34 Ma. However, their $\delta^{13}\text{C}$ data series is not yet available for independent analysis.

As previously mentioned, we had constructed a ~ 19.3 Myr-long ATS of the Lightness series of the 8.39–135 m interval from the Late Volgian to Barremian from the IKU-6814/04-U-02 drilled core in the Greenland-Norwegian Seaway ([Fig. 10B, Table 5](#)). Based on the Greenland-Norwegian Seaway biostratigraphy, the estimated duration is ~ 6.75 Myr for Berriasian Stage (70.7–135 m), a ~ 7.29 Myr duration for combined Valanginian and Hauterivian stages (35.8–70.7 m), and ~ 5.27 Myr duration for the Barremian Stage (8–35.8 m) ([Fig. 10B](#)). A duration of 5.13 ± 0.34 Myr for the Barremian Stage was also estimated by [Fiet and Gorin \(2000\)](#) from their analysis of a cyclic carbonate-dominated

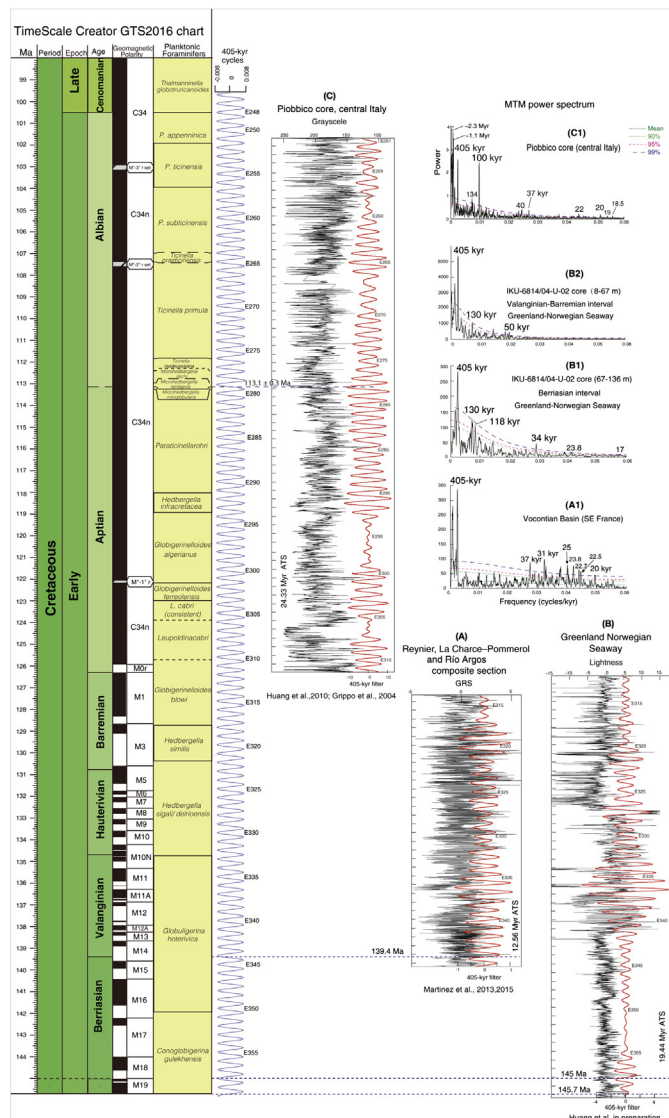


Figure 10 Our restudy and 405-kyr tuning of selected series for the Early Cretaceous ATS. Chronostratigraphy columns on the left were generated using TimeScale Creator 7.0 (engineering.purdue.edu/Stratigraphy/tscreator) with the GTS2016 integrated stratigraphy (Ogg et al., 2016). (A) GRS residuals series (after subtracting a 15% weighted average) from the Vocontian Basin (SE France) (the original data from Martinez et al. (2013, 2015), using the 405 kyr period to tune the 442.93 m composite section from the Reynier, La Charce—Pommerol and Río Argos three cores). (B) Lightness residuals series (after subtracting a 15% weighted average) of the IKU-6814/04-U-02 core in

pelagic sequence in the Umbria-Marche Basin (central Italy), and a similar 5.2 Myr minimum duration was estimated by Amodio et al. (2013) from the shallow-marine carbonates of the two drilled cores in the central Apennines (central Italy) and one outcrop section at Monte Faito in the southern Apennines (southern Italy). Although we could not define the exactly position for the Valanginian/Hauterivian boundary in our data set, if we assume an age of 145.8 or 145 Ma for the Jurassic/Cretaceous boundary, then the top of Barremian stage age is at about 126.5 Ma based on the \sim 19.3 Myr ATS. Therefore, there is significant agreement on the combined duration for the Berriasian through Barremian stages of the Early Cretaceous, even though the actual stages have not yet been officially defined by GSSPs. This total Berriasian-Barremian cycle-scaled duration was implicitly incorporated into GTS2016 to assign approximate ages for the common Tethyan stage boundary usage relative to an age of 126.3 ± 0.4 Ma for the Barremian/Aptian boundary (Ogg et al., 2012b). This \sim 19.3 Myr-long Greenland-Norwegian ATS and the corresponding Berriasian-Barremian stae interval could be assigned as the 405-kyr chrono-cycles from E360 to E312 (Fig. 10B).

The Aptian and Albian stages have been studied for cyclostratigraphy in Italian sections and boreholes. The most important, but also controversial, cyclostratigraphy study was the 12.9 Myr-long ATS interpreted for the Aptian stage in the Piobbico core that was drilled in the Fucoid Marls at Piobbico (central Italy) by Huang et al. (2010), which used as the reference scale for Aptian events in GTS2012 and GTS2016 (Ogg et al., 2012b; 2016). This ATS was based on the 405-kyr long-eccentricity cycle tuning of the high-resolution grayscale series of the 33.7 m of Aptian in that core that was well-dated by calcareous nannofossils, planktonic foraminifers and organic-rich episodes. The Piobbico core did not recover the basal-Aptian interval of magnetic chron M0r, therefore the Aptian ATS was extended by the \sim 0.5 Myr duration for the M0r zone based on the correlation with the Cismon core to yield an the entire Aptian stage duration of about 13.4 Myr. Even though this 13.4 Myr-long Piobbico core ATS for the

the Greenland-Norwegian Seaway (the original data download from <http://doi.pangaea.de/10.1594/PANGAEA.141090> posted by Swientek (2004)). (C) Grayscale residuals series (after subtracting a 15% weighted average) of Piobbico core (central Italy) (the original data from Huang et al. (2010) and Grippo et al. (2004), for the entire 77-m-long Piobbico core grayscale series). All the 405 kyr filter output (red curve, passband: 0.00247 ± 0.0006 cycles/kyr). A1-C1 are 2π MTM power spectrum of A-C series.

Table 5 Reanalysis of Selected Early Cretaceous Reference Sections Using Standardized Tuning to 405-kyr Long-Eccentricity Cycle and MTM Power-Spectra Analysis. Span (Myr) and Age Limits (Ma) are Based on the Interpreted Tuning Results

Location	Geologic-age	Data source	Proxy	Span (Myr)	Significant spectral cycles (kyr)	Assigned E-cycles	Age limits (Ma)
Reynier, La Charce—Pommerol and Río Argos composite core (Southern Spain)	Uppermost Berriasian-upper Barremian	Martinez et al. (2013), (2015)	GRS	12.56	E: 405 (tuned) O: 37, 31 P: 25, 23.8, 22.7, 22.5, 20	E345-E314	139.88–127.32
Greenland Norwegian Seaway	Uppermost Tithonian–upper Barremian	Huang et al. (preparation)	Lightness	19.44	405 e: 130, 118 O: 34 P: 23.8, 17	E360-E312	145.94–126.5
Piobbico core (central Italy)	Basal Aptian–uppermost Albian	Huang et al. (2010), Grayscale Grippo et al. (2004)	Grayscale	24.5	405 e: 134, 100 O: 40, 37 P: 22, 20, 19, 18.5	E311.5-E251	126.3–101.8

Aptian stage is much longer than the 6.4 ± 0.2 Myr duration estimated by Fiet (2000) from the nearby outcrop or the 6.8 ± 0.4 Myr duration estimated by Fiet et al. (2006) from the cyclostratigraphic study in the Vocontian basin (SE of France), it is consistent with 13.8 Myr duration estimated by Al-Husseini and Matthews (2010) based on the Arabian sequence stratigraphy scaled to their 405 kyr “straton” chronology.

For the Albian Stage, Grippo et al. (2004) constructed a 12.4 Myr-long ATS (including three 405 kyr missing in the top of the core and therefore spliced from an outcrop study) based on the 405-kyr long-eccentricity cycle tuning of the 43 m high-resolution grayscale series of the same Piobbico core. This Albian Piobbico ATS is longer than the duration of 10.64 Myr estimated from the Col de Palluel section of Rosans in Hautes-Alpes (France) by Gale et al. (2011).

We combined these two cyclostratigraphic studies for the entire 77-m-long Piobbico core plus the Chron M0r part of the Cismon core to derive a 25.8 Myr-long ATS spanning the Aptian and Albian stages (Fig. 10C, Table 5). The Aptian/Albian boundary interval has a U-Pb date of 113.1 ± 0.3 Ma on a basal Albian volcanic ash layer in the northwest Germany (Selby et al., 2009), and the corresponding biostratigraphic boundary is known in the Piobbico core. Therefore, the calculated base of the Aptian age of 126.5 Ma in this restudy does not alter the 126.3 ± 0.4 Ma in GTS2012 and GTS2016, and calculated the Albian/Cenomanian boundary age of about 100.485 Ma is identical to the radiometric dating of 100.5 ± 0.4 Ma used GTS2012 and GTS2016. The entire 24.4 Myr-long Piobbico core ATS reference section could be assigned as the 405-kyr chrono-cycles from E311.5 to E251 (Fig. 10C).

It should be noted that the age model used for the Late Jurassic through Early Cretaceous in GTS2016 is undergoing revision; partly from the apparent discrepancies between its reliance on published radiometric dates on oceanic basalts drilled by the Ocean Drilling Program (ODP) and some significantly younger new U-Pb dates from volcanic ash beds in the Neuquén Basin of Argentina (e.g., Vennari et al., 2014; Aguirre-Urreta et al., 2015) and elsewhere (e.g., Midtkandal et al., 2016). For example, an ID-TIMS U-Pb date of 139.55 ± 0.18 Ma occurring in the middle of the regional *Argentiniceras noduliferum* ammonite zone (Vennari et al., 2014) has been correlated to lowermost Chron M16r (Kietzmann et al., 2018, this volume), at a level that had been assigned an approximate age of 142 Ma in GTS2016. Therefore, even though the cycle-derived durations of most of the Oxfordian through Barremian stages as summarized

in this current study are similar to the stage-durations estimated in GTS2016, then either the GTS2016 scale must be shifted nearly 2 Myr younger, which would imply either lengthening one or more of the Middle Jurassic stages which have conflicting cycle-derived durations while shortening the Aptian Stage or with some other method of compensation. At this point, there are not enough reliable and verified cyclostratigraphic studies on Middle Jurassic or on Aptian sections a lack of independent radioisotopic ages to resolve these inconsistencies among published interpretations and dating.

5.2 The Late Cretaceous

The Late Cretaceous includes **Cenomanian, Turonian, Coniacian, Santonian, Campanian and Maastrichtian stages** and spans about 34 Myr from ~ 100 Ma at Early/Late Cretaceous boundary to ~ 66 Ma at Cretaceous/Paleogene boundary. There are nearly 40 cyclostratigraphic studies published for the Late Cretaceous over the past twenty years (Batenburg et al., 2012; 2014; 2016; 2017; Chen et al., 2015; Eldrett et al., 2015; Friedrich et al., 2016; Gale, 1995; Gale et al., 2002; Hennebert et al., 2009; Hilgen, 2010; Husson et al., 2011; 2014; Jung et al., 2013; Kuiper et al., 2008; Lanci et al., 2010; Laurin et al., 2014, 2016; Li et al., 2017; Locklair and Sageman, 2008; Ma et al., 2014; Meyers et al., 2012; Mitchell et al., 2008; Perdiou et al., 2016; Prokoph et al., 2001; Sageman et al., 2006, 2014; Sprovieri et al., 2013; Thibault et al., 2012a,b, 2016a,b; Voigt et al., 2008; Voigt and Schönfeld., 2010; Wu et al., 2009, 2013; 2014; Westerhold et al., 2008) (Fig. 9).

The important Late Cretaceous reference section spanning ~ 200 -m in the Bottaccione Gorge region in the Umbria–Marche Basin (Gubbio, central Italy) was used by Sprovieri et al. (2013) to construct a ~ 23 Myr-long high-resolution $\delta^{13}\text{C}_{\text{carb}}$ (~ 20 cm sample interval) series. The lower part of section is recorded pelagic sequence with the light gray to light green limestones interbedded bands of black chert in the Scaglia Bianca Formation from the late Albian to early Turonian age. There is ~ 1 m-thick of black laminated shales interbedded with gray radiolarian sands known as the Bonarelli Level (considered as OAE2) in the late Cenomanian at the uppermost of the Scaglia Bianca Formation. The Scaglia Rossa Formation in the upper part of the section consists of pink clay-rich limestones and cherts variations. Sprovieri et al. (2013) derived durations of 5.40, 4. Myr, 3.46 and 2.94 Myr for the Cenomanian, Turonian, Coniacian and Santonian stage, respectively. We re-analyzed their data and recognized 55 cycles of ~ 3.44 – 4.88 m wavelengths to construct a 22.275 Myr-long ATS based

on tuning these ~ 4 m cycles to the stable 405-kyr long-eccentricity cycles (Fig. 11A, Table 6). Anchoring this to the radioisotopic and astrochronologic intercalibration date of 93.9 ± 0.15 Ma for the Cenomanian/Turonian boundary (Bonarelli Level) (Meyers et al., 2012), then this 22.275 Myr-long Bottaccione $\delta^{13}\text{C}_{\text{carb}}$ ATS spans 101.2 to 78.94 Ma and could be assigned as the 405-kyr chrono-cycles from E249 to E195 (Fig. 11A).

This cycle-tuning of the Tethyan-based carbon-isotope record can be verified and extended upward using the $\delta^{13}\text{C}_{\text{carb}}$ series data from Jarvis et al. (2002), who presented a 467.3-m thick $\delta^{13}\text{C}_{\text{carb}}$ series from the Tethyan pelagic-hemipelagic section near El Kef of the northern Tunisia spanning Campanian to basal Maastrichtian. We re-analyzed the available $\delta^{13}\text{C}_{\text{carb}}$ from the Table 1 in the Jarvis et al. (2002) paper. The power spectral of this $\delta^{13}\text{C}_{\text{carb}}$ series display significant peaks at ~ 45 , ~ 13 and ~ 5 m wavelengths. We constructed a 6.952 Myr-long ATS based on tuning the ~ 45 m cycles to the 405-kyr long-eccentricity (Fig. 11G, Table 6). When we anchor the Campanian/Maastrichtian boundary at 476 m to its estimated age of 72.1 Ma, this 6.95 Myr-long ATS spans 78.88 to 71.94 Ma and could be assigned as the 405-kyr chrono-cycles from E195 to E178 (Fig. 11G). Combined with the 22.275 Myr-long $\delta^{13}\text{C}$ ATS constructed from the Umbria-Marche Basin (Gubbio, central Italy), a 29 Myr-long $\delta^{13}\text{C}_{\text{carb}}$ ATS could be compiled spanning most of the Cenomanian through Maastrichtian stages that could be assigned as the 405-kyr chrono-cycles from E250 to E178.

The coeval succession of Upper Cretaceous chalk-marl alternations in the Western Interior Seaway of North America are the main reference sections for intercalibration of radiometric ages to biostratigraphic zones and carbon-isotope excursions. Joo and Sageman (2014) compiled a composite carbon isotope record for the Cenomanian-Campanian from well-defined biostratigraphic cores (Aristocrat Angus (AA), Portland (PO) and CL-1). A ~ 14 Myr-long $\delta^{13}\text{C}_{\text{org}}$ time scale has been constructed based on the Meyers et al. (2012) and Sageman et al. (2014) intercalibrated astrochronologic and radioisotopic ($^{40}\text{Ar}/^{39}\text{Ar}$ and U-Pb) ages of 93.90 ± 0.15 Ma, 89.75 ± 0.38 Ma, 86.49 ± 0.44 Ma and 84.19 ± 0.38 Ma for the Cenomanian/Turonian, Turonian/Coniacian, Coniacian/Santonian and Santonian/Campanian boundaries, respectively. Spectral analysis of this $\delta^{13}\text{C}_{\text{org}}$ time series shows strong peaks at 120, ~ 200 , 360, 500, ~ 900 and ~ 1500 kyr. The 360 and 500 kyr peaks should be 405 kyr period in the astronomical theory. We used the composite section (2140.8–2417.6 m) from the AA,

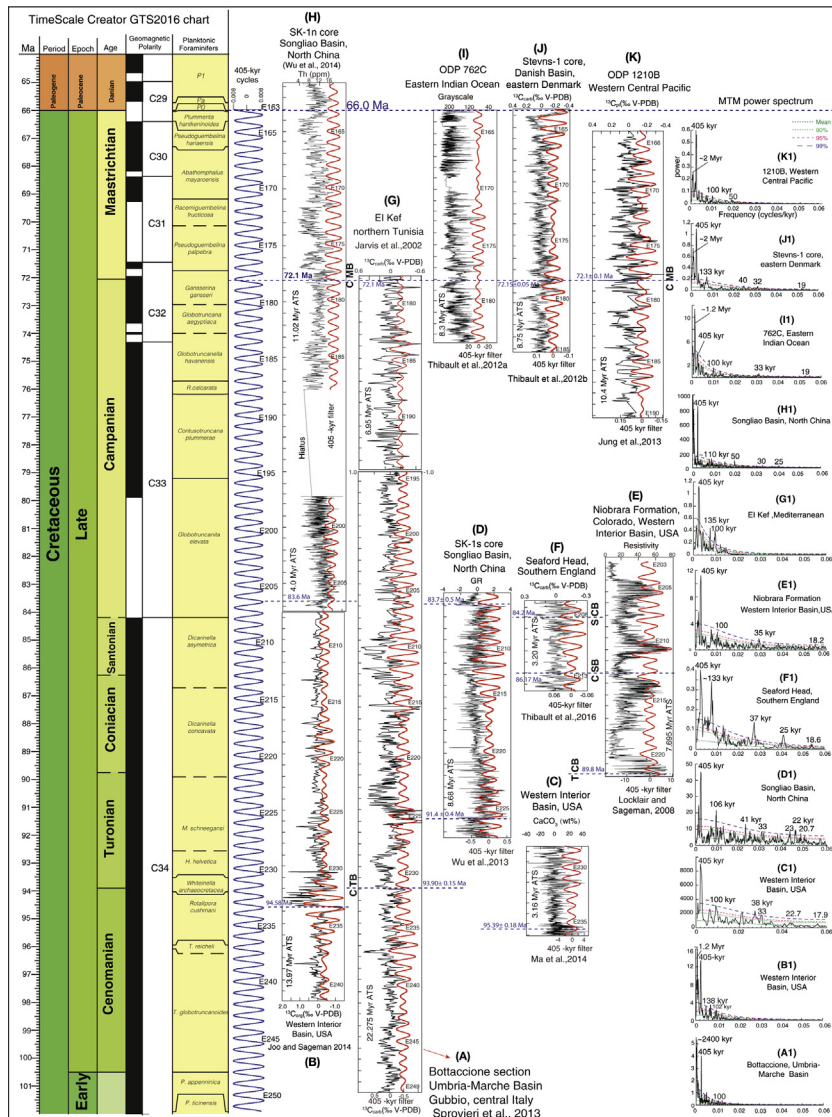


Figure 11 Our restudy and 405-kyr tuning of selected series for the Late Cretaceous ATS. Chronostratigraphy columns on the left were generated using TimeScale Creator 7.0 (engineering.purdue.edu/Stratigraphy/tscreator) with the GTS2016 integrated stratigraphy (Ogg et al., 2016). (A) $\delta^{13}\text{C}_{\text{carb}}$ residuals series (after subtracting a 15% weighted average) of the Bottaccione section in the Umbria-Marche Basin (the original data from Sprovieri et al., 2013). (B) $\delta^{13}\text{C}_{\text{org}}$ residuals series (after subtracting a 6% weighted average) of the Western Interior Basin (USA) (the original data from Joo and Sageman, 2014). (C) CaCO_3 (wt%) residuals series (after subtracting a 10% weighted average) of the Western Interior Basin (USA) (the original data from Ma et al., 2014).

PO and CL-1 cores and recognized 36 cycles with ~ 7 m thickness that is compares well with the 33 cycles from the $\delta^{13}\text{C}_{\text{org}}$ time series of 83.8–97.235 Ma obtained by band-passing for 325–524 kyr cycles (filter frequency from 0.00187 to 0.00307). Tuning these 36 cycles of ~ 7 m as 405-kyr long-eccentricity cycles, then a 14.58 Myr-long ATS has been constructed (Fig. 11B, Table 6). Anchoring with a 94.58 Ma age for the base of the OAE2 (Joo and Sageman, 2014), then this 14.58 Myr-long ATS spans 97.97 to 83.39 Ma. This 13.97 Myr-long $\delta^{13}\text{C}_{\text{org}}$ ATS from 97.97 to 84.0 Ma could be assigned as the 405-kyr chrono-cycles from E241 to E207 (Fig. 11 B).

The Cenomanian/Turonian boundary interval in this Western Interior Seaway region has been studied at very high resolution by Ma et al. (2014). They obtained high-resolution (5 mm) X-ray fluorescence (XRF) core scanning data including the weight percent CaCO_3 series and a ${}^{40}\text{Ar}/{}^{39}\text{Ar}$ age of 95.39 ± 0.18 Ma from bentonites in the *Dunveganoceras pondi* ammonite biozone in the uppermost Lincoln Limestone Member of the Aristocrat Angus core. When constrained by two ${}^{40}\text{Ar}/{}^{39}\text{Ar}$ ages of 93.79 ± 0.26 and 94.20 ± 0.28 Ma for the *Watinoceras devonense* and *Sciponoceras gracile* ammonite biozones (Meyers et al., 2012), the cyclostratigraphy indicates a strong precessional control on the deposition of the organic-carbon-rich strata. We re-tuned the CaCO_3 series using the 405-kyr long-eccentricity cycles to construct a ~ 3.16 Myr ATS. This was anchored to 95.39 Ma at the ~ 2304 m level in the Angus core

(D) GR residuals series (after subtracting a 30% weighted average) of the SK-I south borehole in the Songliao Basin (NE China) (the original data from Wu et al., 2013). (E) Resistivity residuals series (after subtracting a 10% weighted average) of the two wells from the Western Interior basin (Colorado, USA) (the original data from Locklair and Sageman, 2008). (F) $\delta^{13}\text{C}_{\text{carb}}$ residuals series (after subtracting a 10% weighted average) of the Seaford Head (southern England) and Bottaccione (central Italy) (the original data from Thibault et al., 2016a). (G) $\delta^{13}\text{C}_{\text{carb}}$ residuals series (after subtracting a 15% weighted average) near El Kef (Mediterranean, northern Tunisia) (the original data from Jarvis et al., 2002). (H) Th series of SK-I south borehole in the Songliao Basin (NE China) (the original data from Wu et al., 2014). (I) Grayscale residuals series (after subtracting a 10% weighted average) of the ODP 762C borehole (the original data from Thibault et al., 2012a). (J) $\delta^{13}\text{C}_{\text{carb}}$ residuals series (after subtracting a 10% weighted average) of the Stevns-1 core of the Danish Basin (eastern Denmark) (the original data from Thibault et al., 2012b). (K) $\delta^{13}\text{C}_{\text{pl}}$ residuals series (after subtracting a 10% weighted average) of the ODP 1210B borehole (the original data from Jung et al., 2012). All the 405 kyr filter output (red curve, passband: 0.00247 ± 0.0003 – 0.0006 cycles/kyr). A1-K1 are 2π MTM power spectrum of A-K series.

Table 6 Reanalysis of Selected Late Cretaceous Reference Sections Using Standardized Tuning to 405-kyr Long-Eccentricity Cycle and MTM Power-Spectra Analysis. Span (Myr) and Age Limits (Ma) are Based on the Interpreted Tuning Results

Location	Geologic-age	Data source	Proxy	Span (Myr)	Significant spectral cycles (kyr)	Assigned E-cycles	Age limits (Ma)
Bottaccione section, Umbria-Marche Basin (central Italy)	Uppermost Albian-lower Campanian	Sprovieri et al. (2013)	$\delta^{13}\text{C}_{\text{carb}}$ (‰)	22.275	E: 405 (tuned) e: 100	E249-E194.4	101.2–78.94
El Kef (northern Tunisia)	Middle Campanian-basal Maastrichtian	Jarvis et al. (2002)	$\delta^{13}\text{C}_{\text{carb}}$ (‰)	6.95	405 e: 134, 100 O: 40 , 37 P: 22, 20, 19, 18.5	E195-E178	78.88–71.94
Western Interior Basin (USA)	Lower Cenomanian-basal Campanian	Joo and Sageman (2014)	$\delta^{13}\text{C}_{\text{org}}$ (‰)	13.97	405 e: 138 , 102	E241-E207	97.97–84
Angus core, Western Interior Basin (USA)	Upper Cenomanian-lower Turonian	Ma et al. (2014)	CaCO_3 (wt%)	3.16	405 e: 100 O: 38 , 33 P: 22.7, 17.9	E236-E228	95.6–92.4
SK-1s core, Songliao Basin (north China)	Middle Turonian-basal Campanian	Wu et al. (2013)	GR	8.68	405 e: 106 O: 41 , 33 P: 23, 22 , 20.7	E227.5-E206	92.08–83.4
Colorado, Western Interior Basin (USA)	Uppermost Turonian-lower Campanian	Locklair and Sageman (2008)	Resistivity	7.695	405 e: 100 O: 35 P: 18.2	E222-E203	89.9–82.2

Seaford Head (southern England)	Uppermost Coniacian–lowermost Campanian	Thibault et al. (2016a)	$\delta^{13}\text{C}_{\text{carb}}$ (‰)	3.2	405 e: 133 O: 37 P: 25, 18.6	E214–E207	86.8–83.6
SK-1n core, Songliao Basin (north China)	Basal Campanian–Lower Paleocene	Wu et al. (2014)	Th (ppm)	14 (4 Myr gap)	405 e: 110 O: 50, 30 P: 25	E207–E161	83.9–65
ODP hole 762C (Eastern Indian Ocean)	Upper Campanian–Basal Paleocene	Thibault et al. (2012a)	grayscale	8.3	405 e: 100 O: 33 P: 19	E184–E164	74.3–66
Stevns-1 core (eastern Denmark)	Upper Campanian–Basal Paleocene	Thibault et al. (2012b)	$\delta^{13}\text{C}_{\text{carb}}$ (‰)	8.75	405 e: 133 O: 40, 32 P: 19	E185–E163	74.68–65.93
ODP hole 1210B (Western Central Pacific)	Middle Campanian – uppermost Maastrichtian	Jung et al. (2013)	$\delta^{13}\text{C}_{\text{pl}}$ (‰)	10.35	405 e: 100 O: 50	E190–E165	77.01–66.66

(Fig. 11 C, Table 6). This \sim 3.16 Myr Angus core ATS could be assigned as the 405-kyr chrono-cycles from E236 to E228 (Fig. 11 C).

The Coniacian and Santonian stages have also been analyzed in this Western Interior Seaway region with its well-defined biostratigraphy. Locklair and Sageman (2008) presented a \sim 85-m thick high-resolution borehole resistivity data series from two wells that record a decimeter-scale rhythmic alternations of chalk and marl beds and decameter-scale oscillations of chalky and marly succession in the Niobrara Formation of Colorado. They constructed a \sim 6.1–6.7 Myr ATS based on tuning \sim 1–2 m cycles in the resistivity series to the 95-kyr short-eccentricity and estimated durations of 3.4 ± 0.13 and 2.39 ± 0.15 Myr for the Coniacian and Santonian stages, respectively. However, the power spectral of the 95 kyr tuned series displays an anomalous suite of significant peaks at 696, 370, 236, 140, 120, 95, 71, 44, 38, 31, 21.3, 19.6 and 18.3 kyr periods that is lacking the stable 405 kyr long-eccentricity cycle peak. Therefore, we used the 19 cycles of \sim 3–5 m wavelength that were recognized from the bandpassed \sim 85-m resistivity series of Locklair and Sageman (2008) to construct a 7.695 Myr-long ATS based on tuning these \sim 3–5 m cycles to the 405-kyr long-eccentricity cycles (Fig. 11E, Table 6). This results in estimated durations of 3.66 and 2.6 Myr for Coniacian and Santonian stages, respectively, which is similar to the assigned durations of 3.5 ± 0.4 and 2.6 ± 0.5 Myr for Coniacian and Santonian stages in the GTS2012 that were based on interpolations from radiometric dating (Siewert, 2011; Ogg et al., 2012b). These durations are also consistent with the estimates of 3.46 and 2.94 Myr for the Coniacian and Santonian by Sprovieri et al. (2013) and the calculated durations of 3.26 ± 0.82 and 2.30 ± 0.82 Myr for Coniacian and Santonian stages based on the intercalibration of astrochronologic and $^{40}\text{Ar}/^{39}\text{Ar}$ and U-Pb ages of 89.75 ± 0.38 Ma for the Turonian/Coniacian, 86.49 ± 0.44 Ma for the Coniacian/Santonian, and 84.19 ± 0.38 Ma for the Santonian/Campanian boundary. When we anchor the 89.8 Ma for the Turonian/Coniacian boundary age, this \sim 7.695 Myr-long resistivity ATS could be assigned as the 405-kyr chrono-cycles from E222 to E203 (Fig. 11E).

This late Coniacian to early Campanian time interval was also studied by Thibault et al. (2016a) in marine sections at Seaford Head (southern England) and Bottaccione (central Italy). They compiled a \sim 3.2 Myr ATS based on tuning the high-resolution bulk carbonate carbon isotopes series to the 405-kyr long-eccentricity cycle (Fig. 11F, Table 6). There are five 405 kyr cycles for the Tethyan Santonian based on the \sim 16 m filtered output of the $\delta^{13}\text{C}_{\text{carb}}$ and the global correlation between the Niobrara Formation of the Western Interior Basin (USA) and English Chalk of

Seaford Head of England and La2010 solution (Laskar et al., 2011). They indicated that the 405 kyr filtered output minima of the resistivity series in the Niobrara Formation correlate to the solution 405-kyr long-eccentricity minima and the $\delta^{13}\text{C}_{\text{carb}}$ filtered output maxima in the Seaford Head (Fig. 11E and F). We accepted their age model option 2 and anchoring to the 84.2 Ma age for the Santonian/Campanian boundary, which in turn was based on the 405-kyr long-eccentricity solution curve minima and the cycle-calibrated isotopic-dating at 84.19 ± 0.38 Ma (Sageman et al., 2014). This results in the Coniacian/Santonian boundary is placed at 86.17 Ma. This ~ 3.2 Myr Seaford Head $\delta^{13}\text{C}_{\text{carb}}$ ATS could be assigned as the 405-kyr chrono-cycles from E214 to E207 (Fig. 11F).

The recent drilling of Upper Cretaceous in the Songliao Basin of northeast China has yielded expanded records in a lacustrine succession. Wu et al. (2013) obtained a ~ 950 -m (from 960 to 1910 m depth) thick GR well log from the SK-Is (south) borehole from the dark mudstones intercalated with thin carbonate layers and black shales of the Nenjiang Formation (960 to 1128.17 m depth), brownish-greenish/grayish mudstone and greenish muddy siltstone of the Yaojia Formation (1128.17 to 1285.91 m depth), gray-dark gray-black mudstone interbedded with marlstone and shale in the lower and thin bedded gray siltstone of the upper part of the Qingshankou Formation (1285.91 to 1782.93 m depth), and grayish green or brown mudstone, siltstone and sandstone in the Quantou Formation (1782.93 to 1910.0 m depth). An 8.68 Myr-long ‘absolute’ ATS was constructed for the early Turonian–early Campanian (92.08 to 83.4 Ma) based on tuning ~ 36 – 65 m wavelengths to the 405-kyr long-eccentricity cycles (Fig. 11D, Table 6). Combined with the four SIMS U–Pb zircon radioisotope ages of by 83.7 ± 0.5 Ma at 1019 m, 90.4 ± 0.4 Ma at 1673 m, 90.1 ± 0.6 Ma at 1705 m, and 91.4 ± 0.5 Ma at 1780 m (He et al., 2012), and the magnetic reversal C33r/C34n boundary at 985.95 m assigned as 83.64 Ma by Ogg et al. (2012). This 8.68 Myr-long SK-Is core GR ATS could be assigned as the 405-kyr chrono-cycles from E227.5 to E206 (Fig. 11D).

In a continuation and enhancement of their previous study, Wu et al. (2014) presented a 1541.66 m Th (thorium) series from the SK1n core (north Songke-1 borehole) of the Songliao Basin. The lithology consists of purple–red-gray mudstone and muddy siltstone in the lower Mingshui Formation; greenish gray-black and purple–red mudstone to greyish green muddy siltstone and sandstone in the upper Mingshui Formation; purple–red and black to gray mudstone and clayey siltstone and sandstone in the Sifangtai Formation; and gray to black mudstone to marl and silty mudstone in the lower part, and black mudstone to greyish black sandy mudstone and

gray siltstone interbedded with sandstone in the upper part of the Nenjiang Formation. The significant peaks of power spectra show the cycle wavelengths ratios of $\sim 20:5:2:1$ in Th series that approximately corresponds to the Milankovitch cycles of 405 and ~ 100 kyr eccentricity, 38 kyr obliquity and ~ 20 kyr precession cycles, respectively. A ~ 14 Myr-long ATS has been constructed from 83.9 to 65 Ma based on the Th series maxima of 405 kyr sedimentary cycles filter output tuned to the maxima of the 405 kyr eccentricity solution curve of La2010d (Laskar et al., 2011) (Fig. 11H, Table 6). This was anchored to an initial magnetostratigraphy age control of the Chron C30n/C29r boundary at 66.3 Ma and the Cretaceous/Paleogene (K/Pg) boundary at 66.0 Ma in GTS2012 (Ogg et al., 2012b). The placement of the K/Pg, Campanian-Maastrichtian, Santonian-Campanian boundaries at depths of 318 m, 752.8 m and 1751.1 m, imply ATS ages of 66, 72.1 and 83.6 Ma, respectively. However, a ca. 4-Myr gap at the top of Nenjiang Formation separates this Th ATS series into two parts of 65–76.077 and 79.9–83.917 Ma. In this case, the SK1n ATS could be assigned as a pair of 405-kyr chrono-cycle intervals from E207 to E197 and E188 to E161 (Fig. 11 H).

The Upper Campanian through Maastrichtian interval was also studied by Husson et al. (2011) in a suite of ODP sites. They constructed a ~ 8 Myr-long ATS based on the recognition of the 405-kyr long-eccentricity variation from the high-resolution MS in the Hole 1258A of ODP Leg 207 (Equatorial Atlantic), MS in 1267B of ODP Leg 208 (South Atlantic), grayscale series in the Hole 762C of ODP Leg 122 (Indian Ocean) and in the Hole 525A of DSDP Leg 74 (South Atlantic). By integrating with the magnetostratigraphy and the astronomical eccentricity solution of La2010a, they estimated the cycle-scaled durations of each chron from C32n1n to C29r and proposed an absolute ATS age for the K/Pg boundary as 65.59 ± 0.07 Ma or 66.0 ± 0.07 Ma and for the Campanian/Maastrichtian boundary as 72.34 and 72.75 Ma. The 66.0 Ma age for K/Pg boundary was also the age model in GTS2012 (Ogg et al., 2012b). Thibault et al. (2012a) identified twenty-one $\sim 2\text{--}7$ m cycles in ODP Hole 762C grayscale series. By assigning these as 405-kyr long-eccentricity cycles, they proposed the age for the Campanian/Maastrichtian boundary as 72.15 ± 0.05 Ma and estimated a duration of 6.15 ± 0.05 Myr for the Maastrichtian Stage. We re-tuned this dataset and similarly recognized twenty-one $\sim 2\text{--}7$ m cycles that we assigned as 405-kyr long-eccentricity cycles. The a ~ 8.3 Myr high-resolution grayscale ATS of ODP Hole 762C spans the Late Campanian at 74.3 Ma to the K/Pg boundary of 66 Ma (Fig. 11I, Table 6). This ~ 8.3 Myr grayscale ATS could be assigned as the 405-kyr chrono-cycles from E184 to E164 (Fig. 11I).

This Upper Campanian through Maastrichtian cyclostratigraphy was further verified by Thibault et al. (2012b), who provided a 456-m thick and 1968 samples to construct the high-resolution carbon isotope series of this interval from the Stevns-1 core drilled in the Danish Basin of eastern Denmark. The core records consist of white chalk with several intercalated marly intervals. The age model and Campanian/Maastrichtian boundary was identified between 320–325 m through the correlation of biostratigraphy and negative $\delta^{13}\text{C}_{\text{carb}}$ excursion event between Stevns-1 core and the GSSP section at Tercis les Bains (SW France). Our spectral analysis of this high-resolution carbon isotope series shows ~ 25 m thick cycles predominant through the series. We constructed a ~ 8.75 Myr-long ATS from 74.677 to 65.925 Ma based on tuning this ~ 25 m cycles to the 405-kyr long-eccentricity and anchoring the 321 m at 72.1 Ma (Fig. 11J, Table 6). This ~ 8.75 Myr-long $\delta^{13}\text{C}_{\text{carb}}$ ATS could be assigned as the 405-kyr chrono-cycles from E185 to E163 (Fig. 11J).

The carbon-isotope record from the same time interval was analyzed by Jung et al. (2013) using a high-resolution planktonic foraminifera ($\delta^{13}\text{C}_{\text{pl}}$) data series from the Hole 1210B of ODP Leg 198 in the tropical Pacific Ocean (Shatsky Rise). The age model for $\delta^{13}\text{C}_{\text{pl}}$ data series based on Voigt et al. (2012) enabled a global correlation of high-resolution $\delta^{13}\text{C}$ records for the Late Cretaceous spanning 77.01 to 66.66 Ma. We reanalyzed this $\delta^{13}\text{C}_{\text{pl}}$ series and tuned the dominant ~ 5 m cycles to the 405-kyr long-eccentricity cycles to construct a ~ 10.4 Myr-long ATS. This compares well with the 10.35 Myr duration from the global $\delta^{13}\text{C}$ age model of 77.01–66.66 Ma (Fig. 11K, Table 6). This 10.4 Myr-long ODP Hole 1210B $\delta^{13}\text{C}_{\text{pl}}$ ATS from ODP Hole 1210B could be assigned as the 405-kyr chrono-cycles from E190 to E165 (Fig. 11K).

For a full Late Cretaceous ATS, there still some correlation problems between different paleoclimate proxies due to the anchor/constraint ages uncertainties. In addition, similar paleoclimate proxies for the 405-kyr E cycles, such as the carbon isotopes but when measured from different materials (bulk carbonate, organic matter, plankton foraminifers, etc.), often do not correlate very well (Fig. 11J and K). But, in other cases, the bulk carbonate $\delta^{13}\text{C}_{\text{carb}}$ ATS from the Western Interior Basin (USA) and the organic carbon $\delta^{13}\text{C}_{\text{org}}$ ATS from the Bottaccione reference section (Gubbio, central Italy) do could correlate well (Fig. 11A and B).

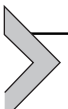
This extensive suite of replicate studies enables coverage and verification of the main 405-kyr tuned ATS for the entire Late Cretaceous (Fig. 11, Table 7). There are at least three ATS sections correlated to each other for the **Turonian**, **Coniacian**, **Santonian** and **Maastrichtian** stages,

Table 7 Summary of the Astronomical Calibrated the Stage Boundary Ages and Durations for the Mesozoic and Compare With the GTS2012

	Stage	Base age (Ma) GTS2012/GTS2016	Duration (Myr)	ATS age (Ma)	ATS duration (Myr)	405-Kyr chrono-cycles
PALE-OGENE	Danian	66.0 ± 0.1		66.0		E163
CRETACEOUS	Maastrichtian	72.1 ± 0.2	6.1	72.1	6.1	E178-E163
	Campanian	83.6 ± 0.3/84.19 ± 0.38	11.5/12.09	84.2	12.1	E208-E178
	Santonian	86.3 ± 0.5/86.49 ± 0.44	2.7/2.3	86.2	2	E213-E208
	Coniacian	89.8 ± 0.4/89.75 ± 0.38	3.5/3.26	89.8	3.6	E221.5-E213
	Turonian	93.9 ± 0.2	4.1/4.15	93.9	4.1	E232-E221.5
	Cenomanian	100.5 ± 0.4	6.6	100.485	6.6	E248-E232
	Albian	113.0 ± 0.4/113.14 ± 0.4	12.5/12.65	113.1	12.6	E279-E248
	Aptian	126.3 ± 0.4	13.3/13.16	126.5	13.4	E311.5-E251
	Barremian	130.8 ± 0.5	4.5			E344-E314
	Hauterivian	133.9 ± 0.6/134.7 ± 0.7	3.1/3.9		5.9	
	Valanginian	139.4 ± 0.7	5.5/4.7	139.4	5.3	
	Berriasian	145.0 ± 0.8/145.7 ± 0.8	5.6/6.3	145.8	6.4	E360-E344
JURASSIC	Tithonian	152.1 ± 0.9	7.1/6.4	152.1	6.3	E376-E360
	Kimmeridgian	157.3 ± 1.0	5.2	157.1	5	E388-E376
	Oxfordian	163.5 ± 1.1/163.1 ± 1.1	6.2/5.8	163.1	6	E403-E388

	Callovian	166.1 ± 1.2	2.6/3.0		<i>E410-E403</i>
	Bathonian	168.3 ± 1.3	2.2	4	<i>E420.6-E410</i>
	Bajocian	170.3 ± 1.4	2.0	170.3	
	Aalenian	$174.1 \pm 1.0/174.2$ ± 1.0	3.8/3.9	174.2	4
	Toarcian	$182.7 \pm 0.7/183.7$ ± 0.5	8.6/9.5	183.7	9.5
	Pliensbachian	$190.8 \pm 1.0/191.4$ ± 0.3	8.1/7.7	192.4	8.7
	Sinemurian	$199.3 \pm 0.3/199.4$ ± 0.3	8.5/8.0	199.430	<i>E429.5-E475</i>
	Hettangian	$201.3 \pm 0.2/201.4$ ± 0.17	2.0/2.0	201.4	1.97
TRIASSIC	Rhaetian	205.4/209.5	4.1/8.2	205.7	4.3
	Norian	221/228.4	15.7/18.9		<i>E585.7-508</i>
	Carnian	237 \pm 1.0	16/8.7	237.0	
	Ladinian	241.5 \pm 1.0	4.5	241.5	4.5
	Anisian	$247.1 \pm 0.1/246.8$ ± 0.2	5.6/5.3	246.8	5.3
	Olenekian	$250 \pm 0.2/249.8 \pm 0.2$	2.9/3.0	249.9	3.1
	Induan	$252.2 \pm 0.2/251.9$ ± 0.02	2.2/2.1	251.9	2

and two ATS sections for most of the **Cenomanian** and the **Campanian** stages. A precise duration for each stage could be obtained based on these ATS reference sections.



6. CONCLUSIONS

In order to calibrate the accurate geological time scale and the accurate durations for each stage, the cyclostratigraphy of multiple sections (marine and continental) correlation need to be developed, carefully cross-correlated and integrated with biostratigraphy, chemostratigraphy, magnetostratigraphy and radioisotopic dating. Also, wherever possible, we need apply the same types of paleoclimate proxies for each section and also compare among different depositional settings (e.g., lacustrine versus marine) and climatic hemispheres. The goal is to recognize the 405-kyr long-eccentricity E cycles and apply tuning to construct the ATS for the Mesozoic with one-to-one correspondence to the predicted astronomical model for these E cycles. Even though this paper mainly focused on the estimates of ages and durations of international geologic stages (Table 1), the main goal of cyclostratigraphy and the ATS is determining the actual rates and precise relative all biologic, geochemical and other events within those stages. Future work needs to focus on closing the main gaps in coverage in the middle Triassic (Ladinian and Carnian stages), the Sinemurian Stage of Early Jurassic, and much of the Middle Jurassic, and verifying the middle Cretaceous (Aptian Stage).

ACKNOWLEDGMENTS

I thank Dr. Mario Sprovieri, Masayuki Ikeda and Huaichun Wu provide their data for this study. I thank Dr. Alessandro Grippo for providing his data from the Aptian-Albian Piobbico core. This work was supported by the National Natural Science Foundation of China (No. 41772029) and Natural Science Foundation for Distinguished Young Scholars of Hubei Province of China (No. 2016CFA051), the 111 Project (No. B14031, B08030), 973 Program (No. 2014CB239101) and the Fundamental Research Funds for the Central Universities, China University of Geosciences (Wuhan) (No. CUGQYZX1705, CUGCJ1703).

REFERENCES

- Ait-Itto, F.Z., Martinez, M., Price, G.D., Addi, A.A., 2018. Synchronization of the astronomical time scales in the Early Toarcian: a link between anoxia, carbon-cycle perturbation, mass extinction and volcanism. *Earth Planet. Sci. Lett.* 493, 1–11.
- Al-Husseini, M., Matthews, R.K., 2010. Tuning Late Barremian – Aptian Arabian Plate and global sequences with orbital periods. *GeoArabia Special Publication 1*, 199–228.

- Algeo, T.J., Hinnov, L., Moser, J., Maynard, J.B., Elswick, E., Kuwahara, K., Sano, H., 2010. Changes in productivity and redox conditions in the Panthalassic Ocean during the latest Permian. *Geology* 38, 187–190.
- Amadio, S., Ferreri, V., D'Argenio, B., 2013. Cyclostratigraphic and chronostratigraphic correlations in the Barremian–Aptian shallow-marine carbonates of the central-southern Apennines (Italy). *Cretac. Res.* 44, 132–156.
- Aguirre-Urreta, B., Lescano, M., Schmitz, M.D., Tunik, M., Concheyro, A., Rawson, P.F., Ramos, V.A., 2015. Filling the gap: new precise Early Cretaceous radioisotopic ages from the Andes. *Geol. Mag.* 152 (3), 557–564. <https://doi.org/10.1017/S001675681400082X>.
- Balog, A., Haas, J., Read, J.F., Coruh, C., 1997. Shallow marine record of orbitally forced cyclicity in a late Triassic carbonate platform, Hungary. *J. Sediment. Res.* 67, 661–675.
- Batenburg, S.J., De Vleeschouwer, D., Sprovieri, M., Hilgen, F.J., Gale, A.S., Singer, B.S., Koeberl, C., Coccioni, R., Claeys, P., Montanari, A., 2016. Orbital control on the timing of oceanic anoxia in the Late Cretaceous. *Clim. Past* 12, 1995–2009.
- Batenburg, S.J., Friedrich, O., Moriya, K., Voigt, S., Cournède, C., Moebius, I., Blum, P., Bornemann, A., Fiebig, J., Hasegawa, T., Hull, P.M., Norris, R.D., Röhl, U., Sexton, P.F., Westerhold, T., Wilson, P.A., Scientists, I.E., 2017. Late Maastrichtian carbon isotope stratigraphy and cyclostratigraphy of the Newfoundland Margin (site U1403, IODP Leg 342). *Newsl. Stratigr.*
- Batenburg, S.J., Gale, A.S., Sprovieri, M., Hilgen, F.J., Thibault, N., Boussaha, M., Orue-Etxebarria, X., 2014. An astronomical time scale for the Maastrichtian based on the Zumaia and Sopelana sections (Basque country, northern Spain). *J. Geol. Soc.* 171, 165–180.
- Batenburg, S.J., Sprovieri, M., Gale, A.S., Hilgen, F.J., Hüsing, S., Laskar, J., Liebrand, D., Lirer, F., Orue-Etxebarria, X., Pelosi, N., Smit, J., 2012. Cyclostratigraphy and astronomical tuning of the Late Maastrichtian at Zumaia (Basque country, northern Spain). *Earth Planet. Sci. Lett.* 359–360, 264–278.
- Benton, M.J., Twitchett, R.J., 2003. How to kill (almost) all life: the end-Permian extinction event. *Trends Ecol. Evol.* 18, 358–365.
- Berger, A., Loutre, M.F., 2004. Astronomical theory of climate change. *J. de Physique IV* 121, 1–35.
- Berger, A.L., 1988. Milankovitch theory and climate. *Rev. Geophys.* 26, 624–657.
- Boulila, S., Galbrun, B., Hinnov, L.A., Collin, P.-Y., 2008a. High-resolution cyclostratigraphic analysis from magnetic susceptibility in a Lower Kimmeridgian (Upper Jurassic) marl–limestone succession (La Méouge, Vocontian Basin, France). *Sediment. Geol.* 203, 54–63.
- Boulila, S., Galbrun, B., Hinnov, L.A., Collin, P.Y., Ogg, J.G., Fortwengler, D., Marchand, D., 2010. Milankovitch and sub-Milankovitch forcing of the Oxfordian (Late Jurassic) Terres Noires Formation (SE France) and global implications. *Basin Res.* 22, 717–732.
- Boulila, S., Galbrun, B., Huret, E., Hinnov, L.A., Rouget, I., Gardin, S., Bartolini, A., 2014. Astronomical calibration of the Toarcian Stage: implications for sequence stratigraphy and duration of the early Toarcian OAE. *Earth Planet. Sci. Lett.* 386, 98–111.
- Boulila, S., Hinnov, L.A., Huret, E., Collin, P.-Y., Galbrun, B., Fortwengler, D., Marchand, D., Thierry, J., 2008b. Astronomical calibration of the early Oxfordian (Vocontian and Paris basins, France): Consequences of revising the Late Jurassic time scale. *Earth Planet. Sci. Lett.* 276, 40–51.
- Brack, P., Mundil, R., Oberli, F., Meier, M., Rieber, H., 1996. Biostratigraphic and radiometric age data question the Milankovitch characteristics of the Latemar cycles (Southern Alps, Italy). *Geology* 24, 371–375.

- Brack, P., Rieber, H., Mundil, R., Blendinger, W., Maurer, F., 2007. Geometry and chronology of growth and drowning of middle Triassic carbonate platforms (Cernera and Bivera/Clapsavon) in the southern Alps (northern Italy). *Swiss J. Geosci.* 100, 327–348.
- Burgess, S.D., Bowring, S., Shen, S.Z., 2014. High-precision timeline for Earth's most severe extinction. *Proc. Natl. Acad. Sci. USA* 111, 3316–3321.
- Burgess, S.D., Muirhead, J.D., Bowring, S.A., 2017. Initial pulse of Siberian Traps sills as the trigger of the end-Permian mass extinction. *Nat. Commun.* 8, 164–169. <https://doi.org/10.1038/s41467-017-00083-9>.
- Channell, J.E.T., Labs, J., Raymo, M.E., 2003. The Réunion Subchronozone at ODP site 981 (Feni Drift, north Atlantic). *Earth Planet. Sci. Lett.* 215, 1–12.
- Charbonnier, G., Boulila, S., Gardin, S., Duchamp-Alphonse, S., Adatte, T., Spangenberg, J.E., Föllmi, K.B., Colin, C., Galbrun, B., 2013. Astronomical calibration of the Valanginian “Weissert” episode: the Orpierre marl–limestone succession (Vocontian Basin, southeastern France). *Cretac. Res.* 45, 25–42.
- Chen, X., Wang, C., Wu, H., Kuhnt, W., Jia, J., Holbourn, A., Zhang, L., Ma, C., 2015. Orbitally forced sea-level changes in the upper Turonian–lower Coniacian of the Tethyan Himalaya, southern Tibet. *Cretac. Res.* 56, 691–701.
- Cheng, L., Wang, J., Wan, Y., Fu, X., Zhong, L., 2017. Astrochronology of the middle Jurassic Buqu Formation (Tibet, China) and its implications for the Bathonian time scale. *Palaeogeogr. Palaeoclimatol. Palaeoecol.* 487, 51–58.
- Clemmanson, L.B., Kent, D.V., Jenkins Jr., F.A., 1998. A Late Triassic lake system in East Greenland: facies, depositional cycles and palaeoclimate. *Palaeocl. Palaeogeo. Palaeoclimatol.* 140, 135–159.
- Cozzi, A., Hinnov, L.A., Hardie, L.A., 2005. Orbitally forced Lofer cycles in the Dachstein Limestone of the Julian Alps (northeastern Italy). *Geology* 33.
- Deng, S., Wang, S., Yang, Z., Lu, Y., Li, X., Hu, Q., An, C., Xi, D., Wan, X., 2015. Comprehensive study of the middle–Upper Jurassic Strata in the Junggar Basin, Xinjiang. *Acta Geoscientica Sinica* 36, 559–574 (In Chinese with English abstract).
- Eldrett, J.S., Ma, C., Bergman, S.C., Lutz, B., Gregory, F.J., Dodsworth, P., Phipps, M., Hardas, P., Minisini, D., Ozkan, A., Ramezani, J., Bowring, S.A., Kamo, S.L., Ferguson, K., Macaulay, C., Kelly, A.E., 2015. An astronomically calibrated stratigraphy of the Cenomanian, Turonian and earliest Coniacian from the Cretaceous western Interior Seaway, USA: implications for global chronostratigraphy. *Cretac. Res.* 56, 316–344.
- Fiet, N., 2000. Calibrage temporel de l'Aptien et des sous-étages associés par une approche cyclostratigraphique appliquée à la série pélagique de Marches-Ombrie, Italie centrale. *Bull. Soc. Géol. Fr.* 171, 103–113.
- Fiet, N., Beaudoin, B., Parize, O., 2001. Lithostratigraphic analysis of Milankovitch cyclicity in pelagic Albian deposits of central Italy: implications for the duration of the stage and substages. *Cretac. Res.* 22, 265–275.
- Fiet, N., Gorin, G., 2000. Lithological expression of Milankovitch cyclicity in carbonate-dominated, pelagic, Barremian deposits in central Italy. *Cretac. Res.* 21, 457–467.
- Fiet, N., Quidelleur, X., Parize, O., Bulot, L., Gillot, P., 2006. Lower Cretaceous stage durations combining radiometric data and orbital chronology: towards a more stable relative time scale? *Earth Planet. Sci. Lett.* 246, 407–417.
- Friedrich, O., Batenburg, S.J., Moriya, K., Voigt, S., Courneéde, C., Möbius, I., Blum, P., Bornemann, A., Fiebig, J., Hasegawa, T., Hull, P.M., Norris, R.D., Röhl, U., Westerhold, T., Wilson, P.A., 2016. Maastrichtian carbon isotope stratigraphy and cyclostratigraphy of the Newfoundland Margin (site U1403, IODP Leg 342). *Clim. Past Discuss.* 1–21.

- Fu, W., Jiang, D.Y., Montanez, I.P., Meyers, S.R., Motani, R., Tintori, A., 2016. Eccentricity and obliquity paced carbon cycling in the Early Triassic and implications for post-extinction ecosystem recovery. *Sci. Rep.* 6, 27793.
- Furin, S., Preto, N., Rigo, M., Roghi, G., Gianolla, P., Crowley, J.L., Bowring, S.A., 2006. Highprecision U-Pb zircon age from the Triassic of Italy: implications for the Triassic time scale and the Carnian origin of calcareous nannoplankton and dinosaurs. *Geology* 34, 1009–1012.
- Gale, A., 1995. Cyclostratigraphy and correlation of the Cenomanian stage in western Europe. *Geol. Soc. Lond. Spec. Publ.* 85, 177–197.
- Gale, A.S., Bown, P., Caron, M., Crampton, J., Crowhurst, S.J., Kennedy, W.J., Petrizzo, M.R., Wray, D.S., 2011. The uppermost Middle and Upper Albian succession at the Col de Palluel, Hautes-Alpes, France: an integrated study (ammonites, inoceramid bivalves, planktonic foraminifera, nanofossils, geochemistry, stable oxygen and carbon isotopes, cyclostratigraphy). *Cretac. Res.* 32, 59–130.
- Gale, A.S., Hardenbol, J., Hathway, B., Kennedy, W.J., Young, J.R., Phansalkar, V., 2002. Global correlation of Cenomanian (Upper Cretaceous) sequences: Evidence for Milankovitch control on sea level. *Geology* 30, 291–294.
- Giraud, F., Beaufort, L., Cotillon, P., 1995. Periodicities of carbonate cycles in the Valanginian of the Vocontian Trough: a strong obliquity control. *Geol. Soc. Lond. Spec. Publ.* 85, 143–164.
- Goldhammer, R.K., Dunn, P., Hardie, L., 1990. Depositional cycles, composite sea-level changes, cycle stacking patterns, and the hierarchy of stratigraphic forcing: examples from Alpine Triassic platform carbonates. *Geol. Soc. Am. Bull.* 102, 535–562.
- Goldhammer, R.K., Dunn, P.A., Hardie, L.A., 1987. High frequency glacio-eustatic sealevel oscillations with Milankovitch characteristics recorded in Middle Triassic platform carbonates in northern Italy. *Am. J. Sci.* 287, 853–892.
- Gradstein, F.M., Ogg, J.G., Smith, A.G., 2004. *A Geologic Time Scale 2004*. Cambridge University Press, Cambridge.
- Gradstein, F.M., 2012. Introduction. In: Gradstein, F.M., Ogg, J.G., Schmitz, M.D., Ogg, G.M. (Eds.), *The Geologic Time Scale 2012*. Elsevier B. V., Amsterdam, pp. 1–29.
- Grippo, A., Fischer, A.G., Hinnov, L.A., Herbert, T.D., Premoli Silva, I., 2004. Cyclostratigraphy and chronology of the Albian stage (Piobbico core, Italy). In: D'Argenio, B., Fischer, A.G., Premoli Silva, I., Weissert, H., Ferreri, V. (Eds.), *Cyclostratigraphy: Approaches and Case Histories*. Society for Sedimentary Geology Special Publication, pp. 57–81.
- Guo, G., Tong, J., Zhang, S., Zhang, J., Bai, L., 2008. Cyclostratigraphy of the induan (early Triassic) in West Pingdingshan section, Chaohu, Anhui province. *Sci. China Ser. D-Earth Sci.* 51, 22–29.
- Hansen, H.J., Lojen, S., Toft, P., Dolence, T., Tong, J., Michaelsen, P., 2000. Magnetic susceptibility and organic carbon isotopes of sediments across some marine and terrestrial Permo-Triassic boundaries. In: Yin, H., Dickins, J.M.R., Tong, J. (Eds.), *Permian-Triassic Evolution of Tethys and Western Circum Pacific*. Elsevier, Amsterdam, pp. 271–289.
- Hardie, L.A., Hinnov, L.A., Brack, P., Mundil, R., Oberli, F., Meier, M., Rieber, H., 1997. Biostratigraphic and radiometric age data question the Milankovitch characteristics of the Latemar cycle (southern Alps, Italy): Comment and reply. *Geology* 25, 470–472.
- Hennebert, M., Robaszynski, F., Goolaerts, S., 2009. Cyclostratigraphy and chronometric scale in the Campanian – Lower Maastrichtian: the Abiod Formation at Ellès, central Tunisia. *Cretac. Res.* 30, 325–338.
- Hilgen, F.J., 2010. Astronomical dating in the 19th century. *Earth-Science Rev.* 98, 65–80.

- Hinnov, L.A., Goldhammer, R.K., 1991. Spectral analysis of the middle Triassic Latemar limestone. *J. Sediment. Res.* 61, 1173–1193.
- Hinnov, L.A., Hilgen, F.J., 2012. Cyclostratigraphy and astrochronology. In: Gradstein, F., Ogg, J., Ogg, G., Smith, D. (Eds.), *The Geologic Time Scale 2012*. Elsevier B.V., Amsterdam, pp. 63–83.
- Hinnov, L.A., Park, J.J., 1999. Strategies for assessing early-middle (Pliensbachian–Aalenian) Jurassic cyclochronologies. *Philosophical Trans. R. Soc. Lond.* 357, 1831–1859.
- Huang, C., Hesselbo, S.P., 2014. Pacing of the Toarcian oceanic anoxic event (early Jurassic) from astronomical correlation of marine sections. *Gondwana Res.* 25, 1348–1356.
- Huang, C., Hesselbo, S.P., Hinnov, L., 2010a. Astrochronology of the late Jurassic Kimmeridge clay (Dorset, England) and implications for earth system processes. *Earth Planet. Sci. Lett.* 289, 242–255.
- Huang, C., Hinnov, L., Fischer, A.G., Grippo, A., Herbert, T., 2010b. Astronomical tuning of the Aptian Stage from Italian reference sections. *Geology* 38, 899–902.
- Huang, C., Hinnov, L.A., Swientek, O., Smelror, M., 2010c. Astronomical Tuning of Late Jurassic–early Cretaceous Sediments (Volgian–ryazanian Stages), Greenland–Norwegian Seaway. AAPG Annual Convention, New Orleans, LA.
- Huang, C., Tong, J., Hinnov, L., Chen, Z.Q., 2011. Did the great dying of life take 700 k.y.? Evidence from global astronomical correlation of the Permian–Triassic boundary interval. *Geology* 39, 779–782.
- Huang, Z., Ogg, J., Gradstein, F., 1993. A quantitative study of Lower Cretaceous cyclic sequences from the Atlantic ocean and the Vocontian Basin (SE France). *Paleoceanography* 8, 275–291.
- Huret, E., Hinnov, L.A., Galbrun, B., Collin, P.-Y., Gardin, S., Rouget, I., 2008. Astronomical calibration and correlation of the Lower Jurassic, Paris and Lombard basins (Tethys). In: 33rd International Geological Congress, Oslo, Norway.
- Hüsing, S.K., Beniest, A., van der Boon, A., Abels, H.A., Deenen, M.H.L., Ruhl, M., Krijgsman, W., 2014. Astronomically-calibrated magnetostratigraphy of the Lower Jurassic marine successions at St. Audrie's Bay and East Quantoxhead (Hettangian–Sinemurian; Somerset, UK). *Palaeogeogr. Palaeoclimatol. Palaeoecol.* 403, 43–56.
- Hüsing, S.K., Deenen, M.H.L., Koopmans, J.G., Krijgsman, W., 2011. Magnetostratigraphic dating of the proposed Rhaetian GSSP at Steinbergkogel (Upper Triassic, Austria): implications for the Late Triassic time scale. *Earth Planet. Sci. Lett.* 302, 203–216.
- Husson, D., Galbrun, B., Laskar, J., Hinnov, L.A., Thibault, N., Gardin, S., Locklair, R.E., 2011. Astronomical calibration of the Maastrichtian (Late Cretaceous). *Earth Planet. Sci. Lett.* 305, 328–340.
- Husson, D., Thibault, N., Galbrun, B., Gardin, S., Minnelli, F., Sageman, B., Huret, E., 2014. Lower Maastrichtian cyclostratigraphy of the Bidart section (Basque Country, SW France): a remarkable record of precessional forcing. *Palaeogeogr. Palaeoclimatol. Palaeoecol.* 395, 176–197.
- Ikeda, M., Bôle, M., Baumgartner, P.O., 2016. Orbital-scale changes in redox condition and biogenic silica/detrital fluxes of the Middle Jurassic Radiolarite in Tethys (Sogno, Lombardy, N-Italy): possible link with glaciation? *Palaeogeogr. Palaeoclimatol. Palaeoecol.* 457, 247–257.
- Ikeda, M., Hori, R.S., 2014. Effects of Karoo–Ferrar volcanism and astronomical cycles on the Toarcian oceanic anoxic events (early Jurassic). *Palaeogeogr. Palaeoclimatol. Palaeoecol.* 410, 134–142.
- Ikeda, M., Tada, R., 2014. A 70 million year astronomical time scale for the deep-sea bedded chert sequence (Inuyama, Japan): implications for Triassic–Jurassic geochronology. *Earth Planet. Sci. Lett.* 399, 30–43.

- Ikeda, M., Tada, R., Ozaki, K., 2017. Astronomical pacing of the global silica cycle recorded in Mesozoic bedded cherts. *Nat. Commun.* 8, 15532.
- Ikeda, M., Tada, R., Sakuma, H., 2010. Astronomical cycle origin of bedded chert: a middle Triassic bedded chert sequence, Inuyama, Japan. *Earth Planet. Sci. Lett.* 297, 369–378.
- Jarvis, I., Mabrouk, A., Moody, R.T.J., Cabrera, S.D., 2002. Late Cretaceous (Campanian) carbon isotope events, sea-level change and correlation of the Tethyan and Boreal realms. *Palaeogeogr. Palaeoclimatol. Palaeoecol.* 188, 215–248.
- Joo, Y.J., Sageman, B.B., 2014. Cenomanian to Campanian carbon isotope chemostratigraphy from the western Interior Basin, U.S.A. *J. Sediment. Res.* 84, 529–542.
- Jung, C., Voigt, S., Friedrich, O., 2012. High-resolution carbon-isotope stratigraphy across the Campanian–Maastrichtian boundary at Shatsky Rise (tropical Pacific). *Cretaceous Res.* 37, 177–185.
- Jung, C., Voigt, S., Friedrich, O., Koch, M.C., Frank, M., 2013. Campanian–Maastrichtian ocean circulation in the tropical Pacific. *Paleoceanography* 28, 562–573.
- Kemp, D.B., Coe, A.L., 2007. A nonmarine record of eccentricity forcing through the Upper Triassic of southwest England and its correlation with the Newark Basin astronomically calibrated geomagnetic polarity time scale from North America. *Geology* 35, 991–994.
- Kemp, D.B., Coe, A.L., Cohen, A.S., Weedon, G.P., 2011. Astronomical forcing and chronology of the early Toarcian (Early Jurassic) oceanic anoxic event in Yorkshire, UK. *Paleoceanography* 26.
- Kent, D.V., Muttoni, G., Brack, P., 2004. Magnetostratigraphic confirmation of a much faster tempo for sea-level change for the Middle Triassic Latemar platform carbonates. *Earth Planet. Sci. Lett.* 228, 369–377.
- Kent, D.V., Olsen, P.E., 2008. Early Jurassic magnetostratigraphy and paleolatitudes from the Hartford continental rift basin (eastern North America): Testing for polarity bias and abrupt polar wander in association with the central Atlantic magmatic province. *J. Geophys. Res. Solid Earth* (1978–2012) 113.
- Kent, D.V., Olsen, P.E., Muttoni, G., 2017. Astrochronostratigraphic polarity time scale (APTS) for the Late Triassic and Early Jurassic from continental sediments and correlation with standard marine stages. *Earth-Science Rev.* 166, 153–180.
- Kietzmann, D.A., Palma, R.M., Iglesia Llanos, M.P., 2015. Cyclostratigraphy of an orbitally-driven Tithonian–Valanginian carbonate ramp succession, southern Mendoza, Argentina: implications for the Jurassic–Cretaceous boundary in the Neuquén Basin. *Sediment. Geol.* 315, 29–46.
- Kietzmann, D.A., Iglesia Llanos, M.P., Kohan Martinez, M., 2018. This volume. Astronomical calibration of the Upper Jurassic – Lower Cretaceous in the Neuquén Basin, Argentina: a contribution from the southern hemisphere to the geologic time scale. In: *Stratigraphy and Time Scales*, vol. 3. Elsevier Publ. (this volume).
- Kuiper, K., Deino, A., Hilgen, F., Krijgsman, W., Renne, P., Wijbrans, J., 2008. Synchronizing rock clocks of Earth history. *Science* 320, 500–504.
- Lanci, L., Muttoni, G., Erba, E., 2010. Astronomical tuning of the Cenomanian Scaglia Bianca Formation at Furlo, Italy. *Earth Planet. Sci. Lett.* 292, 231–237.
- Laskar, J., Fienga, A., Gastineau, M., Manche, H., 2011. La2010: a new orbital solution for the long-term motion of the Earth. *Astron. Astrophys.* 532.
- Laskar, J., Robutel, P., Joutel, F., Gastineau, M., Correia, A., Levrard, B., 2004. A long-term numerical solution for the insolation quantities of the Earth. *Astron. Astrophys.* 428, 261–285.
- Laurin, J., Čech, S., Uličný, D., Štaffen, Z., Svobodová, M., 2014. Astrochronology of the Late Turonian: implications for the behavior of the carbon cycle at the demise of peak greenhouse. *Earth Planet. Sci. Lett.* 394, 254–269.

- Laurin, J., Meyers, S.R., Galeotti, S., Lanci, L., 2016. Frequency modulation reveals the phasing of orbital eccentricity during Cretaceous Oceanic Anoxic Event II and the Eocene hyperthermals. *Earth Planet. Sci. Lett.* 442, 143–156.
- Lefranc, M., Beaudoin, B., Chilès, J.P., Guillemot, D., Ravenne, C., Trouiller, A., 2008. Geostatistical characterization of Callovo–Oxfordian clay variability from high-resolution log data. *Phys. Chem. Earth, Parts A/B/C* 33, S2–S13.
- Lehrmann, D.J., Ramezani, J., Bowring, S.A., Martin, M.W., Montgomery, P., Enos, P., Payne, J.L., Orchard, M.J., Hongmei, W., Jiayong, W., 2006. Timing of recovery from the end-Permian extinction: Geochronologic and biostratigraphic constraints from south China. *Geology* 34, 1053–1056.
- Lehrmann, D.J., Stepchinski, L., Altiner, D., Orchard, M.J., Montgomery, P., Enos, P., Ellwood, B.B., Bowring, S.A., Ramezani, J., Wang, H., Wei, J., Yu, M., Griffiths, J.D., Minzoni, M., Schaal, E.K., Li, X., Meyer, K.M., Payne, J.L., 2015. An integrated biostratigraphy (conodonts and foraminifers) and chronostratigraphy (paleomagnetic reversals, magnetic susceptibility, elemental chemistry, carbon isotopes and geochronology) for the Permian–Upper Triassic strata of Guandao section, Nanpanjiang Basin, south China. *J. Asian Earth Sci.* 108, 117–135.
- Li, M., Huang, C., Hinnov, L., Chen, W., Ogg, J., Tian, W., 2018. Astrochronology of the Anisian stage (middle Triassic) at the Guandao reference section, south China. *Earth Planet. Sci. Lett.* 482, 591–606.
- Li, M., Ogg, J., Zhang, Y., Huang, C., Hinnov, L., Chen, Z.-Q., Zou, Z., 2016. Astronomical tuning of the end-Permian extinction and the early Triassic Epoch of south China and Germany. *Earth Planet. Sci. Lett.* 441, 10–25.
- Li, M., Zhang, Y., Huang, C., Ogg, J., Hinnov, L., Wang, Y., Zou, Z., Li, L., Grasby, S., Zhong, Y.J., Huang, K.K., 2017b. Astronomical tuning and magnetostratigraphy of the Upper Triassic Xujiahe Formation of south China and Newark Supergroup of North America: implications for the Late Triassic time scale. *Earth Planet. Sci. Lett.* 475, 207–223.
- Li, M., Zhang, Y., Huang, C., Ogg, J., Hinnov, L., Wang, Y., Zou, Z., Li, L., 2017c. Astrochronology and magnetostratigraphy of the Xujiahe Formation and Newark Supergroup: implications for the Late Triassic time scale. AGU Abstr.
- Li, Y.-X., Montañez, I.P., Liu, Z., Ma, L., 2017. Astronomical constraints on global carbon-cycle perturbation during Oceanic Anoxic Event 2 (OAE2). *Earth Planet. Sci. Lett.* 462, 35–46.
- Liu, Z., Liu, X., Huang, S., 2017. Cyclostratigraphic analysis of magnetic records for orbital chronology of the Lower Cretaceous Xiagou Formation in Linze, northwestern China. *Palaeogeogr. Palaeoclimatol. Palaeoecol.* 481, 44–56.
- Locklair, R.E., Sageman, B.B., 2008. Cyclostratigraphy of the Upper Cretaceous Niobrara Formation, Western Interior, U.S.A.: A Coniacian–Santonian orbital timescale. *Earth Planet. Sci. Lett.* 269, 540–553.
- Ma, C., Meyers, S.R., Sageman, B.B., Singer, B.S., Jicha, B.R., 2014. Testing the astronomical time scale for oceanic anoxic event 2, and its extension into Cenomanian strata of the Western Interior Basin (USA). *Geol. Soc. Am. Bull.* 126, 974–989.
- Maron, M., Rigo, M., Bertinelli, A., Katz, M.E., Godfrey, L., Zaffani, M., Muttoni, G., 2015. Magnetostratigraphy, biostratigraphy, and chemostratigraphy of the Pignola–Abriola section: New constraints for the Norian–Rhaetian boundary. *Geol. Soc. Am. Bull.* 127, 962–974.
- Martinez, M., Deconinck, J.-F., Pellenard, P., Reboulet, S., Riquier, L., 2013. Astrochronology of the Valanginian Stage from reference sections (Vocontian Basin, France) and palaeoenvironmental implications for the Weisser Event. *Palaeogeogr. Palaeoclimatol. Palaeoecol.* 376, 91–102.

- Martinez, M., Deconinck, J.-F., Pellenard, P., Riquier, L., Company, M., Reboulet, S., Moiroud, M., 2015. Astrochronology of the Valanginian–Hauterivian stages (Early Cretaceous): Chronological relationships between the Paraná–Etendeka large igneous province and the Weissert and the Faraoni events. *Glob. Planet. Change* 131, 158–173.
- Martinez, M., Krencker, F.-N., Mattioli, E., Bodin, S., 2017. Orbital chronology of the Pliensbachian – Toarcian transition from the Central High Atlas Basin (Morocco). *Newsl. Stratigr.* 50, 47–69.
- Martinez, M., Pellenard, P., Deconinck, J.F., Monna, F., Riquier, L., Boulila, S., Moiroud, M., Company, M., 2012. An orbital floating time scale of the Hauterivian/Barremian GSSP from a magnetic susceptibility signal (Río Argos, Spain). *Cretac. Res.* 36, 106–115.
- Maurer, F., Hinnov, L., Schlager, W., 2004. Statistical time-series analysis and sedimentological tuning of bedding rhythms in a Triassic basinal succession (Southern Alps, Italy). In: Cyclostratigraphy: Approaches and Case Histories, pp. 83–99.
- Mazza, M., Rigo, M., 2012. Taxonomy and biostratigraphic record of the Upper Triassic conodonts of the Pizzo Mondello section (Western Sicily, Italy), GSSP candidate for the base of the Norian. *Riv. Ital. Paleontol. Stratigr.* 118 (1), 85–130.
- Meyers, S.R., Siewert, S.E., Singer, B.S., Sageman, B.B., Condon, D.J., Obradovich, J.D., Jicha, B.R., Sawyer, D.A., 2012. Intercalibration of radioisotopic and astrochronologic time scales for the Cenomanian-Turonian boundary interval. *West. Inter. Basin USA. Geol.* 40, 7–10.
- Midtkandal, I., Svensen, H.H., Planke, S., Corfu, F., Polteau, S., Torsvik, T.H., Faleide, J.I., Gundvag, S.-A., Selnes, H., Kürschner, W., Olaussen, S., 2016. The Aptian (Early Cretaceous) oceanic anoxic event (OAE1a) in Svalbard, Barents Sea, and the absolute age of the Barremian-Aptian boundary. *Palaeogeogr. Palaeoclimatol. Palaeoecol.* 463, 126–135.
- Mietto, P., Manfrin, S., Preto, N., Rigo, M., Roghi, G., Furin, S., Gianolla, P., Posenato, R., Muttoni, G., Nicora, A., Buratti, N., Cirilli, S., Spötl, C., Ramezani, J., Bowring, S.A., 2012. The Global Boundary Stratotype Section and Point (GSSP) of the Carnian Stage (Late Triassic) at Prati di Stuores/Stuores Wiesen Section (Southern Alps, NE Italy). *Episodes* 35, 414–430.
- Milankovitch, M., 1941. Kanon der Erdbestrahlung und seine Anwendung auf das Eiszeitenproblem (1998 reissue in English: Canon of Insolation and the Ice-Age Problem). Royal Serbian Academy, Section of Mathematical and Natural Sciences, Belgrade.
- Mitchell, R.N., Bice, D.M., Montanari, A., Cleaveland, L.C., Christianson, K.T., Coccioni, R., Hinnov, L.A., 2008. Oceanic anoxic cycles? Orbital prelude to the Bonarelli Level (OAE 2). *Earth Planet. Sci. Lett.* 267, 1–16.
- Müller, T., Price, G.D., Bajnai, D., Nyerges, A., Kesjár, D., Raucsik, B., Varga, A., Judik, K., Fekete, J., May, Z., Pálfy, J., Hesselbo, S., 2017. New multiproxy record of the Jenkyns Event (also known as the Toarcian Oceanic Anoxic Event) from the Mecsek Mountains (Hungary): Differences, duration and drivers. *Sedimentology* 64, 66–86.
- Mundil, R., Brack, P., Meier, M., Rieber, H., Oberli, F., 1996. High resolution U-Pb dating of Middle Triassic volcaniclastics: Time-scale calibration and verification of tuning parameters for carbonate sedimentation. *Earth Planet. Sci. Lett.* 141, 137–151.
- Mundil, R., Zühlke, R., Bechstädt, T., Peterhänsel, A., Egenhoff, S.O., Oberli, F., Meier, M., Brack, P., Rieber, H., 2003. Cyclicity in Triassic Platform Carbonates: Synchronizing Radio-Isotopic and Orbital Clocks. *Terra Nova* 15, 81–87.
- Muttoni, G., Kent, D.V., Olsen, P.E., Di Stefano, P., Lowrie, W., Bernasconi, S.M., Hernández, F.M., 2004. Tethyan magnetostratigraphy from Pizzo Mondello (Sicily) and correlation to the Late Triassic Newark astrochronological polarity time scale. *Geol. Soc. Am. Bull.* 116, 1043.

- Ogg, J., Ogg, G., Gradstein, F., 2016. A Concise Geologic TimeScale 2016. Elsevier, Amsterdam.
- Ogg, J.G., Hinnov, L.A., Huang, C., Jurassic, 2012a. In: Gradstein, F.M., Ogg, J.G., Schmitz, M., Ogg, G. (Eds.), The Geologic Time Scale 2012. Elsevier, pp. 793–853.
- Ogg, J.G., Hinnov, L.A., Huang, C., Cretaceous, 2012b. In: Gradstein, F.M.O., Ogg, J.G., Schmitz, M., Ogg, G. (Eds.), The Geologic Time Scale 2012. Elsevier, pp. 731–791.
- Olsen, P.E., Kent, D.V., 1996. Milankovitch Climate forcing in the tropics of Pangaea during the late Triassic. *Palaeogeogr. Palaeoclimatol. Palaeoecol.* 122, 1–26.
- Olsen, P.E., Kent, D.V., 1999. Long-period Milankovitch cycles from the Late Triassic and Early Jurassic of eastern North America and their implications for the calibration of the Early Mesozoic time-scale and the long-term behaviour of the planets. *Philosophical Trans. R. Soc. A Math. Phys. Eng. Sci.* 357, 1761–1786.
- Olsen, P.E., Kent, D.V., Whiteside, J.H., 2011. Implications of the Newark Supergroup-based astrochronology and geomagnetic polarity time scale (Newark-APTS) for the tempo and mode of the early diversification of the Dinosauria. *Earth Environ. Sci. Trans. R. Soc. Edinburgh* 101, 201–229.
- Ovtcharova, M., Bucher, H., Schaltegger, U., Galfetti, T., Brayard, A., Guex, J., 2006. New Early to Middle Triassic U–Pb ages from South China: Calibration with ammonoid biochronozones and implications for the timing of the Triassic biotic recovery. *Earth Planet. Sci. Lett.* 243, 463–475.
- Ovtcharova, M., Goudemand, N., Hammer, Ø., Guodun, K., Cordey, F., Galfetti, T., Schaltegger, U., Bucher, H., 2015. Developing a strategy for accurate definition of a geological boundary through radio-isotopic and biochronological dating: The Early–Middle Triassic boundary (South China). *Earth-Science Rev.* 146, 65–76.
- Paillard, D., Labeyrie, L., Yiou, P., 1996. Macintosh Program Performs Time-Series Analysis, *Eos, Trans. AGU* 77, 379.
- Perdiou, A., Thibault, N., Anderskou, K., van Buchem, F., Arie Buijs, G.J., Bjerrum, C.J., 2016. Orbital calibration of the late Campanian carbon isotope event in the North Sea. *J. Geol. Soc.* 173, 504–517.
- Preto, N., Hinnov, L.A., 2003. Unraveling the origin of carbonate platform cycloths in the Upper Triassic Durrenstein Formation (Dolomites, Italy). *J. Sediment. Res.* 73, 774–789.
- Preto, N., Hinnov, L.A., Hardie, L.A., De Zanche, V., 2001. Middle Triassic orbital signature recorded in the shallow-marine Latemar carbonate buildup (Dolomites, Italy). *Geology* 29, 1123–1126.
- Preto, N., Hinnov, L.A., Zanche, V.D., Mietto, P., Hardie, L.A., 2004. The Milankovitch interpretation of the Latemar platform cycles (Dolomites, Italy): implications for geochronology, biostratigraphy, and Middle Triassic carbonate accumulation. In: Publication, S.S. (Ed.), Cyclostratigraphy: Approaches and Case Histories. Society for Sedimentary Geology, pp. 167–182.
- Prokoph, A., Villeneuve, M., Agterberg, F.P., Rachold, V., 2001. Geochronology and calibration of global Milankovitch cyclicity at the Cenomanian-Turonian boundary. *Geology* 29, 523–526.
- Rampino, M.R., Prokoph, A., Adler, A., 2000. Tempo of the end-Permian event: high-resolution cyclostratigraphy at the Permian–Triassic boundary. *Geology* 28, 643–646.
- Rodriguez-Tovar, F.J., Pardo-Iguzquiza, E., Reolid, M., Bartolini, A., 2016. Spectral analysis of Toarcian sediments from the Valdorbia section (Umbria-Marche Apennines): the astronomical input in the foraminiferal record. *Res. Paleontol. Stratigraphy* 12, 187–197.
- Ruebsam, W., Münzberger, P., Schwark, L., 2014. Chronology of the Early Toarcian environmental crisis in the Lorraine Sub-Basin (NE Paris Basin). *Earth Planet. Sci. Lett.* 404, 273–282.

- Ruhl, M., Deenen, M., Abels, H., Bonis, N., Krijgsman, W., Kürschner, W., 2010. Astronomical constraints on the duration of the early Jurassic Hettangian stage and recovery rates following the end-Triassic mass extinction (St Audrie's Bay/East Quantoxhead, UK). *Earth Planet. Sci. Lett.* 295, 262–276.
- Ruhl, M., Hesselbo, S.P., Hinnov, L., Jenkyns, H.C., Xu, W., Riding, J.B., Storm, M., Minisini, D., Ullmann, C.V., Leng, M.J., 2016. Astronomical constraints on the duration of the Early Jurassic Pliensbachian Stage and global climatic fluctuations. *Earth Planet. Sci. Lett.* 455, 149–165.
- Sageman, B.B., Meyers, S.R., Arthur, M.A., 2006. Orbital time scale and new C-isotope record for Cenomanian-Turonian boundary stratotype. *Geology* 34, 125–128.
- Sageman, B.B., Singer, B.S., Meyers, S.R., Siewert, S.E., Walaszczyk, I., Condon, D.J., Jicha, B.R., Obradovich, J.D., Sawyer, D.A., 2014. Integrating $^{40}\text{Ar}/^{39}\text{Ar}$, U-Pb, and astronomical clocks in the Cretaceous Niobrara Formation, Western Interior Basin, USA. *Geol. Soc. Am. Bull.* 126, 956–973.
- Selby, D., Mutterlose, J., Condon, D.J., 2009. U–Pb and Re–Os geochronology of the Aptian/Albian and Cenomanian/Turonian stage boundaries: Implications for timescale calibration, osmium isotope seawater composition and Re–Os systematics in organic-rich sediments. *Chemical Geology* 265, 394–409.
- Schoene, B., Guex, J., Bartolini, A., Schaltegger, U., Blackburn, T.J., 2010. Correlating the end-Triassic mass extinction and flood basalt volcanism at the 100 ka level. *Geology* 38, 387–390.
- Sha, J., Olsen, P.E., Pan, Y., Xu, D., Wang, Y., Zhang, X., Yao, X., Vajda, V., 2015. Triassic–Jurassic climate in continental high-latitude Asia was dominated by obliquity-paced variations (Junggar Basin, Ürümqi, China). *Proc. Natl. Acad. Sci. USA* 112, 3624–3629.
- Schaller, M.F., Wright, J.D., Kent, D.V., 2015. A 30 Myr record of Late Triassic atmospheric pCO_2 variation reflects a fundamental control of the carbon cycle by changes in continental weathering. *Geol. Soc. Am. Bull.* 127, 661–671.
- Shen, C., Schoepfer, S.D., Henderson, C.M., 2017. Astronomical tuning of the Early Triassic Induan Stage in the distal Montney Formation, NE British Columbia, Canada. *Geol. Soc. Am.* 49 (6) <https://doi.org/10.1130/abs/2017AM-300972>. gsa.confex.com/gsa/2017AM/webprogram/Paper300972.html.
- Shen, S.Z., Bowring, S.A., 2014. The end-Permian mass extinction: a still unexplained catastrophe. *Nat. Sci. Rev.* 1, 492–495.
- Shen, S.-Z., Ramezani, J., Chen, J., Cao, C.-Q., Erwin, D.H., Zhang, H., Xiang, L., Schoepfer, S.D., Henderson, C.M., Zheng, Q.-F., Bowring, S.A., Wang, Y., Li, X.-H., Wang, X.-D., Yuan, D.-X., Zhang, Y.-C., Mu, L., Wang, J., Wu, Y.-S., 2018. A sudden end-Permian mass extinction in South China. *Geol. Soc. Am. Bull.* in press.
- Siewert, S.E., 2011. Integrating $^{40}\text{Ar}/^{39}\text{Ar}$, U–pb and Astronomical Clocks in the Cretaceous Niobrara Formation. University of Wisconsin at Madison, p. 74 (M.S. thesis).
- Spahn, Z.P., Kodama, K.P., Preto, N., 2013. High-resolution estimate for the depositional duration of the Triassic Latemar Platform: A new magnetostratigraphy and magnetic susceptibility cyclostratigraphy from basinal sediments at Rio Sacuz, Italy. *Geochem. Geophys. Geosys.* 14, 1245–1257.
- Sprenger, A., Ten Kate, W.G., 1993. Orbital forcing of calcilutite–marl cycles in southeast Spain and an estimate for the duration of the Berriasian stage. *Geol. Soc. Am. Bull.* 105, 807–818.
- Sprovieri, M., Coccioni, R., Lirer, F., Pelosi, N., Lozar, F., 2006. Orbital tuning of a lower Cretaceous composite record (Maiolica Formation, central Italy). *Paleoceanography* 21.

- Sprovieri, M., Sabatino, N., Pelosi, N., Batenburg, S.J., Coccioni, R., Iavarone, M., Mazzola, S., 2013. Late Cretaceous orbitally-paced carbon isotope stratigraphy from the Bottaccione Gorge (Italy). *Palaeogeogr. Palaeoclimatol. Palaeoecol.* 379–380, 81–94.
- Strasser, A., 2007. Astronomical time scale for the Middle Oxfordian to Late Kimmeridgian in the Swiss and French Jura Mountains. *Swiss J. Geosci.* 100, 407–429.
- Suan, G., Mattioli, E., Pittet, B., Lécuyer, C., Sucheras-Marx, B., Duarte, L.V., Philippe, M., Reggiani, L., Martineau, F., 2010. Secular environmental precursors to Early Toarcian (Jurassic) extreme climate changes. *Earth Planet. Sci. Lett.* 290, 448–458.
- Sucheras-Marx, B., Giraud, F., Fernandez, V., Pittet, B., Lécuyer, C., Olivero, D., Mattioli, E., 2013. Duration of the Early Bajocian and the associated $\delta^{13}\text{C}$ positive excursion based on cyclostratigraphy. *J. Geol. Soc.* 170, 107–118.
- Swientek, O., 2002. The Greenland Norwegian Seaway: Climatic and Cyclic Evolution of Late Jurassic-early Cretaceous Sediments. PhD Thesis. Mathematisch-Naturwissenschaftliche Fakultät der Universität zu Köln, p. 119.
- Swientek, O., 2004. Lightness of Sediment Core IKU-6814/04-U-02. PANGAEA. <https://doi.org/10.1594/PANGAEA.141090>.
- Szuradies, M., 2004. Magnetostratigraphy: the key to a global correlation of the classic Germanic Trias-case study Volpriehausen Formation (Middle Buntsandstein), Central Germany. *Earth Planet. Sci. Lett.* 227, 395–410.
- Szuradies, M., Bachmann, G.H., Menning, M., Nowaczyk, N.R., Kaeding, K.C., 2003. Magnetostratigraphy and high-resolution lithostratigraphy of the Permian–Triassic boundary interval in central Germany. *Earth Planet. Sci. Lett.* 212, 263–278.
- Szuradies, M., Geluk, M.C., Krijgsman, W., Kürschner, W.M., 2012. The continental Permian–Triassic boundary in the Netherlands: Implications for the geomagnetic polarity time scale. *Earth Planet. Sci. Lett.* 317, 165–176.
- Thibault, N., Harlou, R., Schovsbo, N., Schiøler, P., Minoletti, F., Galbrun, B., Lauridsen, B.W., Sheldon, E., Stemmerik, L., Surlyk, F., 2012a. Upper Campanian–Maastrichtian nannofossil biostratigraphy and high-resolution carbon-isotope stratigraphy of the Danish Basin: Towards a standard $\delta^{13}\text{C}$ curve for the Boreal Realm. *Cretac. Res.* 33, 72–90.
- Thibault, N., Husson, D., Harlou, R., Gardin, S., Galbrun, B., Huret, E., Minoletti, F., 2012b. Astronomical calibration of upper Campanian–Maastrichtian carbon isotope events and calcareous plankton biostratigraphy in the Indian Ocean (ODP Hole 762C): Implication for the age of the Campanian–Maastrichtian boundary. *Palaeogeogr. Palaeoclimatol. Palaeoecol.* 337–338, 52–71.
- Thibault, N., Galbrun, B., Gardin, S., Minoletti, F., Le Callonnec, L., 2016a. The end-Cretaceous in the southwestern Tethys (Elles, Tunisia): orbital calibration of paleoenvironmental events before the mass extinction. *Int. J. Earth Sci.* 105, 771–795.
- Thibault, N., Jarvis, I., Voigt, S., Gale, A.S., Attree, K., Jenkyns, H.C., 2016b. Astronomical calibration and global correlation of the Santonian (Cretaceous) based on the marine carbon isotope record. *Paleoceanography* 31, 847–865.
- Tian, S., Chen, Z.-Q., Huang, C., 2014. Orbital Forcing and Sea-Level Changes in the Earliest Triassic of the Meishan Section, South China. *J. Earth Sci.* 25, 64–73.
- Vennari, V.V., Lescano, M., Naipauer, M., Aguirre-Urreta, B., Concheyro, A., Schaltegger, U., Armstrong, R., Pimentel, M., Ramos, V.A., 2014. New constraints on the Jurassic–Cretaceous boundary in the High Andes using high-precision U-Pb data. *Gondwana Res.* 26, 374–385.
- Voigt, S., Erbacher, J., Mutterlose, J., Weiss, W., Westerhold, T., Wiese, F., Wilmsen, M., Wonik, T., 2008. The Cenomanian – Turonian of the Wunstorf section – (North Germany): global stratigraphic reference section and new orbital time scale for Oceanic Anoxic Event 2. *Newsl. Stratigr.* 43, 65–89.

- Voigt, S., Gale, A.S., Jung, C., Jenkyns, H.C., 2012. Global correlation of Upper Campanian – Maastrichtian successions using carbon-isotope stratigraphy: development of a new Maastrichtian timescale. *Newsl. Stratigr.* 45, 25–53.
- Voigt, S., Schönfeld, J., 2010. Cyclostratigraphy of the reference section for the Cretaceous white chalk of northern Germany, Lägerdorf–Kronsmoor: A late Campanian–early Maastrichtian orbital time scale. *Palaeogeogr. Palaeoclimatol. Palaeoecol.* 287, 67–80.
- Vollmer, T., Werner, R., Weber, M., Tougiannidis, N., Roehling, H.-G., Hambach, U., 2008. Orbital control on Upper Triassic playa cycles of the Steinmergel-Keuper (Norian): A new concept for ancient playa cycles. *Palaeogeogr. Palaeoclimatol. Palaeoecol.* 267, 1–16.
- Waterhouse, H.K., 1999. Orbital forcing of palynofacies in the Jurassic of France and the United Kingdom. *Geology* 27, 511–514.
- Weedon, G., Jenkyns, H., 1999. Cyclostratigraphy and the Early Jurassic timescale: data from the Belemnite Marls, Dorset, southern England. *Geol. Soc. Am. Bull.* 111, 1823–1840.
- Weedon, G.P., Coe, A.L., Gallois, R.W., 2004. Cyclostratigraphy, orbital tuning and inferred productivity for the type Kimmeridge Clay (Late Jurassic), Southern England. *J. Geol. Soc.* 161, 655–666.
- Weedon, G.P., Jenkyns, H.C., Coe, A.L., Hesselbo, S.P., 1999. Astronomical calibration of the Jurassic time-scale from cyclostratigraphy in British mudrock formations. *Philosophical Trans. R. Soc. Lond. Ser. A Mathematical, Physical and Engineering Sciences* 357, 1787–1813.
- Westerhold, T., Röhl, U., Raffi, I., Fornaciari, E., Monechi, S., Reale, V., Bowles, J., Evans, H.F., 2008. Astronomical calibration of the Paleocene time. *Palaeogeogr. Palaeoclimatol. Palaeoecol.* 257, 377–403.
- Whiteside, J.H., Olsen, P.E., Eglington, T., Brookfield, M.E., Sambrotto, R.N., 2010. Compound-specific carbon isotopes from Earth's largest flood basalt eruptions directly linked to the end-Triassic mass extinction. *Proc. Natl. Acad. Sci.* 107, 6721–6725.
- Wotzlaw, J.-F., Brack, P., Storck, J.-C., 2018. High-resolution stratigraphy and zircon U–Pb geochronology of the Middle Triassic Buchenstein Formation (Dolomites, northern Italy): precession-forcing of hemipelagic carbonate sedimentation and calibration of the Anisian–Ladinian boundary interval. *J. Geol. Soc.* 175, 71–85.
- Wotzlaw, J.F., Gux, J., Bartolini, A., Gallet, Y., Krystyn, L., McRoberts, C.A., Taylor, D., Schoene, B., Schaltegger, U., 2014. Towards accurate numerical calibration of the Late Triassic: High-precision U–Pb geochronology constraints on the duration of the Rhaetian. *Geology* 42, 571–574.
- Wu, H., Zhang, S., Feng, Q., Jiang, G., Li, H., Yang, T., 2012. Milankovitch and sub-Milankovitch cycles of the early Triassic Daye Formation, South China and their geochronological and paleoclimatic implications. *Gondwana Res.* 22, 748–759.
- Wu, H., Zhang, S., Hinnov, L.A., Jiang, G., Yang, T., Li, H., Wan, X., Wang, C., 2014. Cyclostratigraphy and orbital tuning of the terrestrial upper Santonian–Lower Danian in Songliao Basin, northeastern China. *Earth Planet. Sci. Lett.* 407, 82–95.
- Wu, H., Zhang, S., Jiang, G., Hinnov, L., Yang, T., Li, H., Wan, X., Wang, C., 2013. Astrochronology of the Early Turonian–Early Campanian terrestrial succession in the Songliao Basin, northeastern China and its implication for long-period behavior of the Solar System. *Palaeogeogr. Palaeoclimatol. Palaeoecol.* 385, 55–70.
- Wu, H., Zhang, S., Jiang, G., Huang, Q., 2009. The floating astronomical time scale for the terrestrial Late Cretaceous Qingshankou Formation from the Songliao Basin of Northeast China and its stratigraphic and paleoclimate implications. *Earth Planet. Sci. Lett.* 278, 308–323.

- Yin, H., Zhang, K., Tong, J., Yang, Z., Wu, S., 2001. The global stratotype section and point (GSSP) of the Permian–Triassic boundary. *Episodes* 24, 102–114.
- Zhang, Y., Li, M., Ogg, J.G., Montgomery, P., Huang, C., Chen, Z.-Q., Shi, Z., Enos, P., Lehrmann, D.J., 2015. Cycle-calibrated magnetostratigraphy of middle Carnian from South China: Implications for Late Triassic time scale and termination of the Yangtze Platform. *Palaeogeogr. Palaeoclimatol. Palaeoecol.* 436, 135–166.
- Zühlke, R., 2004. Integrated Cyclostratigraphy of a Model Mesozoic Carbonate Platform—the Latemar (Middle Triassic, Italy), Cyclostratigraphy: Approaches and Case Histories. Society for Sedimentary Geology (SEPM), pp. 183–211.
- Zühlke, R., Bechstädt, T., Mundil, R., 2003. Sub-Milankovitch and Milankovitch forcing on a model Mesozoic carbonate platform – the Latemar (Middle Triassic, Italy). *Terra. Nova* 15, 69–80.